Reactions of 6,6'-Bis(*nido*-decaboranyl) Oxide and 6-Hydroxy-*nido*-decaborane with Dihalogenobis(phosphine) Complexes of Nickel, Palladium, and Platinum, and some Related Chemistry; Nuclear Magnetic Resonance Investigations and the Crystal and Molecular Structures of Bis(dimethylphosphine)-di-μ-(2,3,4-η³-*nido*-hexaboranyl)-diplatinum(*Pt–Pt*), $[Pt_2(\mu\text{-}\eta^3\text{-}B_6H_9)_2(PMe_2Ph)_2]$, and of 2,4-Dichloro-1,1-bis(dimethylphenylphosphine)-*closo*-1-nickeladecaborane, $[(PhMe_2P)_2NiB_9H_7Cl_2]$*

Norman N. Greenwood, Michael J. Hails, John D. Kennedy, and Walter S. McDonald
Department of Inorganic and Structural Chemistry, University of Leeds, Leeds LS2 9JT

A modified procedure for the preparation and isolation of 6,6'-$(B_{10}H_{13})_2O$ leads also to the isolation of the new compound 6-$B_{10}H_{13}OH$, which has been fully characterised by ^{11}B and ^1H n.m.r. and mass spectroscopy. The structures and some chemistry of these two related oxyboranes are compared. The reaction of either 6,6'-$(B_{10}H_{13})_2O$ or 6-$B_{10}H_{13}OH$ with *cis*-$[PtCl_2L_2]$ (L = PMe_2Ph or PPh_3) gives three platinaboranes, *arachno*-$[L_2PtB_8H_{12}]$ (**1**), *nido*-$[L_2PtB_{10}H_{12}]$, and $[Pt_2(\mu\text{-}\eta^3\text{-}B_6H_9)_2L_2]$ (**2**). The yellow needles of (**2**) (L = PMe_2Ph) are monoclinic, space group $P2_1/c$, with a = 1 014.0(2), b = 586.8(2), c = 2 316.9(6) pm, β = 91.66(2)°, Z = 2 and the molecular structure is that of a centrosymmetric 14-vertex *arachno*-diplatinaborane in which two B_6H_9 clusters are bonded above and below an almost linear P–Pt–Pt–P system. The bonding of each B_6H_9 unit is symmetrical *trihapto*. In sharp contrast the reaction of 6,6'-$(B_{10}H_{13})_2O$ with the corresponding nickel complex *cis*-$[NiCl_2(PMe_2Ph)_2]$ gives mainly phosphine–boranes of known type, *viz.* $PhMe_2P{\cdot}BH_3$, $PhMe_2P{\cdot}B_3H_7$, and $PhMe_2P{\cdot}B_9H_{13}$, together with a low yield of the new metallaborane *closo*-$[(PhMe_2P)_2NiB_9H_7Cl_2]$ (**3**). The red crystals of (**3**) are monoclinic, space group $C2/c$, with a = 1 341.2(2), b = 1 321.5(2), c = 1 476.3(2) pm, β = 109.50(1)°, Z = 4 and the molecular structure is that of a bicapped square antiprismatic 10-vertex *closo*-nickelaborane in which the $Ni(PMe_2Ph)_2$ group takes up a capping four-connected site. The reaction of 6,6'-$(B_{10}H_{13})_2O$ with *cis*-$[PdCl_2L_2]$ (L = PMe_2Ph or PPh_3) gives phosphine–boranes analogous to those from the reaction with *cis*-$[NiCl_2(PMe_2Ph)_2]$, together with *arachno*-$[L_2PdB_8H_{12}]$, the palladium analogues of (**1**). Treatment of (**1**) with KH followed by *cis*-$[PdCl_2(PMe_2Ph)_2]$ gives the moderately stable heterodimetallaborane cluster compound, $[(PhMe_2P)_4PdPtB_8H_{10}]$, an *arachno*-palladaplatinaborane species and the first metallaborane of any kind to contain metals from two different periods in the Periodic Table. Treatment of (**2**) with base followed by *cis*-$[PtCl_2(PMe_2Ph)_2]$ gives the 15-vertex trimetallaborane cluster compound $[Pt_2(\mu\text{-}\eta^3\text{-}B_6H_9)(\mu\text{-}\{\eta^3\text{-}B_6H_8\text{-}\eta^2\text{-}PtH(PMe_2Ph)_2\})(PMe_2Ph)_2]$. The ^1H, ^{11}B, and ^{31}P n.m.r. behaviour of these compounds have been investigated in detail using both single- and double-resonance techniques, and a number of interesting patterns emerge.

Although many derivatives of binary boron hydrides have been prepared[1,2] much of the chemistry of the derivatives, even of the more common polyhedral boranes, remains unexplored. This paper is concerned with some reactions of two related derivatives of *nido*-decaborane, $B_{10}H_{14}$, namely 6-hydroxy-*nido*-decaborane, $B_{10}H_{13}OH$, and its formal anhydride 6,6'-bis(*nido*-decaboranyl) oxide, $(B_{10}H_{13})_2O$. The bis(decaboranyl) oxide has been known for some time,[3] although it was not thoroughly characterised until recently.[4,5] It is known to undergo degradation to $B_{10}H_{14}$ and $B_9H_{13}L$ (where L = SMe_2 or tetrahydrofuran) under basic conditions, but to be particularly stable to acidic reagents such as HF, BCl_3, PCl_5, PBr_5, H_2SO_4, $SOCl_2$, and Br_2;[3] the rest of its chemistry remains uninvestigated. The hydroxy-compound $B_{10}H_{13}OH$ on the other hand is new. Although we had observed it previously by mass spectrometry as an impurity of low abundance in technical grade *nido*-decaborane[6] its identification was then tentative. We now describe its preparation, isolation, and more thorough characterisation. The bulk of this paper is, however, concerned with the reactions of $B_{10}H_{13}OH$ and of $(B_{10}H_{13})_2O$ with dihalogenobis(phosphine) complexes of platinum(II), palladium(II), and nickel(II), which lead to some interesting metallaborane species; a preliminary report of one aspect of this work has been published,[7] but we present here the results of further work on these systems.

We have used the I.U.P.A.C. recommended numbering convention[8] for the polyhedral systems encountered in this work; these are summarised in structures (**I**)—(**VI**). Structures (**III**) and (**IV**) are the so-called '*iso*' and '*n*' *arachno*-nine-vertex cluster arrangements respectively.

Results and Discussion

1. *Characterisation of* 6-*Hydroxy*-nido-*decaborane and Comparison with* 6,6'-*Bis*(nido-*decaboranyl*) *Oxide*.—As reported some years ago,[3] 6,6'-bis(*nido*-decaboranyl) oxide can be prepared by the action of sulphuric acid on 6,6'-bis(dimethyl sulphide)-*arachno*-decaborane, $B_{10}H_{12}(SMe_2)_2$: a benzene solu-

* *Supplementary data available* (No. SUP 56177, 3 pp.): thermal parameters for $[(PhMe_2P)_2NiB_9H_7Cl_2]$. See Instructions for Authors, *J. Chem. Soc., Dalton Trans.*, 1985, Issue 1, pp. xvii—xix. Structure factors are available from the editorial office.
Non-S.I. unit employed: mmHg ≈ 13.6 × 9.8 Pa.

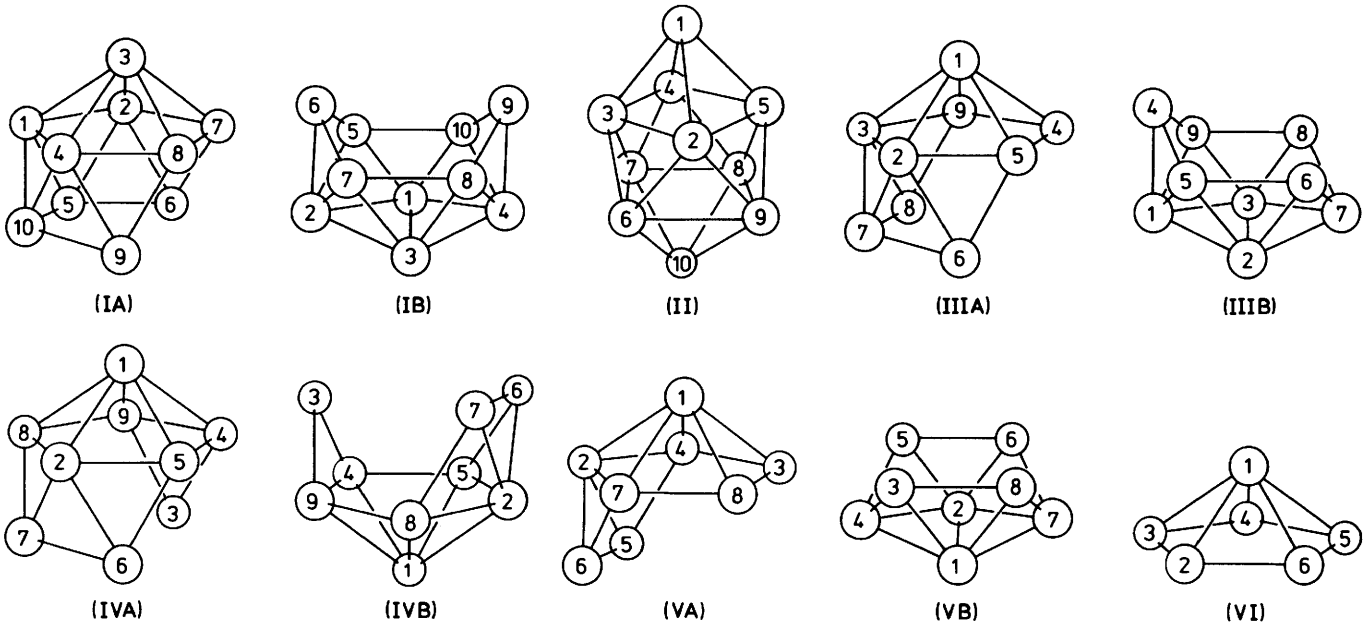

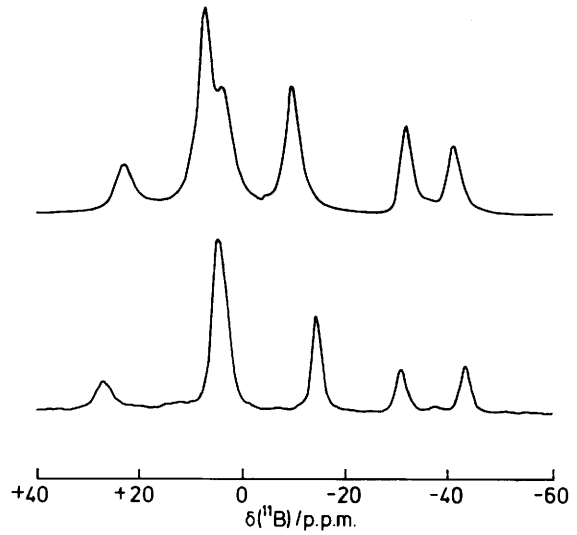

Figure 1. 32-MHz ^{11}B-{^{1}H(broad band noise)} n.m.r. spectra for 6,6′-$(B_{10}H_{13})_2O$ (upper trace) and 6-$B_{10}H_{13}OH$ (lower trace) in $CDCl_3$ solution at +21 °C. In the absence of proton decoupling all resonances, except those at lowest field due to B(6), become doublets with $^{1}J(^{11}B-^{1}H)$ *ca.* 150 Hz

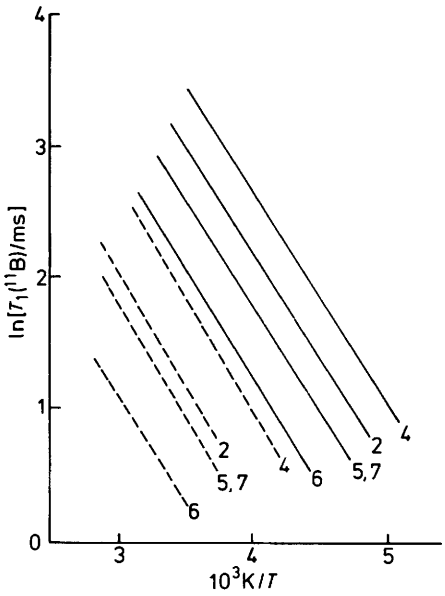

Figure 2. Gross variation with temperature of the longitudinal relaxation times, $T_1(^{11}B)$, of selected boron-11 resonances of $B_{10}H_{13}OH$ in $CDCl_3$ (——) and $(B_{10}H_{13})_2O$ in $CD_3C_6D_5$ (– – –). Numbers refer to atomic positions in the *nido*-decaboranyl skeleton numbered as in structure (**I**)

tion of $B_{10}H_{12}(SMe_2)_2$ is shaken with H_2SO_4 (98%), and removal of the benzene from the organic layer yields an off-white residue from which the product, $(B_{10}H_{13})_2O$, can be removed by exhaustive sublimation at *ca.* 100 °C/0.1 mmHg. This compound has been well characterised by n.m.r. spectroscopy and single-crystal *X*-ray diffraction analysis.[4,5,9] We have now found that extraction of the resulting sublimation residue with hot cyclohexane followed by recrystallisation then yields 6-hydroxy-*nido*-decaborane, $B_{10}H_{13}OH$, as a white crystalline hygroscopic solid, decomp. > 160 °C, in yields of up to *ca.* 26%. [This compound may be related to previously reported[3] products, tentatively formulated at that time as $B_{10}H_{14}O_2$ and $B_{10}H_{14}O$ from analytical and i.r. data.] Sublimation of the initial reaction residue under higher vacuum (*ca.* 10^{-4}—10^{-5} mmHg) leads to cosublimation of the oxide and hydroxide, whereas use of higher pressures and temperatures appears to increase the yield of the oxide at the expense of the hydroxide.

The oxide and hydroxide can be distinguished by i.r. absorption spectroscopy [the hydroxide has ν(OH) = 3 570 cm^{-1}] and their mass spectra are quite different. Both exhibit high mass 'cut-offs' at *m/e* values appropriate to their molecular formulae, and high resolution measurements confirm the constitution of the hydroxide. The fragmentation pattern of the oxide $(B_{10}H_{13})_2O$ exhibits other elements of interest; for example there is a significant incidence of doubly-charged ions at *m/e* = *ca.* 122 and there is an unexpected principal fragmentation to give ions corresponding to $[B_{17}H_n]^+$ at *m/e* = *ca.* 217 which presumably involves the ready loss of B_3H_mO fragments from the $[B_{20}H_pO]^+$ ions.

Table 1. Boron-11 and proton n.m.r. data for 6-$B_{10}H_{13}OH$ and (for comparison) 6,6′-$(B_{10}H_{13})_2O$; $CDCl_3$ solution at +21 °C

								Bridge	
(*a*) 6-$B_{10}H_{13}OH$									
Assignment[a]	1,3	2	4	5,7	6	8,10	9	(5,6)(6,7)	(8,9)(9,10)
$\delta(^{11}B)$/p.p.m.	+6.5[b]	−31.7	−43.7	−13.7	+26.1	+4.3[b]	+5.0[b]		
$\triangle\sigma(^{11}B)$/p.p.m.[c]	+3.5	−3.4	+8.6	+12.9	−13.3	+5.1	+7.8		
$^1J(^{11}B-^1H)$/Hz	150 ± 20	161 ± 10	157 ± 10	147 ± 10	—	150 ± 20	150 ± 20		
$\delta(^1H)$/p.p.m.[d]	+3.44	+1.28	+0.26	+2.13	+4.13 (OH)[e]	+2.94	+3.74	−0.50	−1.74
$\triangle\sigma(^1H)$/p.p.m.[c]	+0.27	−0.63	+0.39	+0.83	—	+0.19	+0.09	−1.59	−0.36
(*b*) 6,6′-$(B_{10}H_{13})_2O$[f]									
$\delta(^{11}B)$/p.p.m.	+5.6[b]	−33.2	−42.5	−10.7	+21.8	+3.0[b]	+7.2[b]		
$\triangle\sigma(^{11}B)$/p.p.m.[c]	+4.4	−1.9	+7.4	+9.9	−9.0	+3.8	+5.6		
$^1J(^{11}B-^1H)$/Hz	145 ± 10	155 ± 10	155 ± 10	150 ± 10	—	145 ± 10	145 ± 10		
$\delta(^1H)$/p.p.m.[d]	+3.29[g]	+1.34	+0.32	+2.45	—	+3.17[g]	+3.91	−0.45	−1.72
$\triangle\sigma(^1H)$/p.p.m.[c]	+0.40	−0.69	+0.23	+0.68	—	−0.04	−0.06	−1.67	−0.42

[a] Based on the assignment for 6,6′-$(B_{10}H_{13})_2O$ (ref. 4). [b] Overlapping resonances distinguished by π-τ-π/2 'partially relaxed' spectroscopy (refs. 4 and 13). [c] $\triangle\sigma$ = substituent shielding effect = $\delta(B_{10}H_{14}) - \delta(B_{10}H_{13}X)$, and is the increase in shielding, σ, for a nucleus in a substituted compound compared to a nucleus in the same site in the unsubstituted species; note that by convention nuclear shielding, σ, and chemical shift, δ, are of opposite sign. [d] Assigned using $^1H-\{^{11}B(selective)\}$ experiments. [e] $\delta(^1H)(OH)$ has considerable solvent dependence: *e.g.* +3.36 p.p.m. in C_6D_6 solution. [f] Data for comparison from ref. 4. [g] Assignments tentative; both the ^{11}B and ^1H resonances for the (1,3) and (8,10) positions are too close for the results of selective $^1H-\{^{11}B\}$ experiments to be conclusive at the field strengths used.

The two compounds can be distinguished by n.m.r. spectroscopy: the 32-MHz ^{11}B n.m.r. spectra of both compounds are shown in Figure 1, and their ^1H and ^{11}B n.m.r. data are summarised in Table 1. It can be seen that the values for both are very similar, the principal differences residing in the somewhat greater substituent chemical-shift effects for the hydroxide compared to the oxide. Interestingly although the β, γ, and δ effects are comparable to those for a 6-chloro-substituent,[10] the α effect is larger than that for chloro, being comparable to that for an alkyl[11] or aryl[12] substituent. However, the differences between the oxide and hydroxide are small, indicating that the electronic effects of the $-OB_{10}H_{13}$ and –OH groups on the 6-position of the *nido*-decaborane cluster are very similar. At 32 MHz the two compounds are best distinguished by their $^{11}B(6)$ resonances at +26.1 and +21.8 p.p.m. for the hydroxide and oxide respectively, which are resolved in mixtures of the two species in common n.m.r. solvents at ambient temperatures; these differences were in fact used to monitor mixtures of the two species in the interconversion investigations discussed below. In addition, the longitudinal (quadrupolar) relaxation times, $T_1(^{11}B)$, are in general longer for the hydroxy-compound than the oxide (Figure 2) under similar solution conditions; this is expected and arises from the smaller molecular size of the hydroxide since the electric-field-gradient tensors at corresponding nuclear positions in the two species must be very similar. The proton n.m.r. spectra for the two compounds are also very similar (Table 1), but in the hydroxide there is an additional signal due to the hydroxy proton, for example at $\delta(^1H)$ = +4.13 p.p.m. in $CDCl_3$ solution at +21 °C. Some fine structure is also apparent arising from homonuclear proton–proton coupling as observed for the corresponding chloride.[13]

The formation of both $(B_{10}H_{13})_2O$ and $B_{10}H_{13}OH$ from the reaction of $B_{10}H_{12}(SMe_2)_2$ with H_2SO_4 warrants some comment. Presumably the reaction has some parallels with the formation of 6-$B_{10}H_{13}Cl$ from the reaction of HCl or $HgCl_2$ with $B_{10}H_{12}(SMe_2)_2$,[14] equation (1). A similar reaction with H_2SO_4 would give the 6-hydrogensulphate [equation (2)] which then presumably yields the two 6-oxydecaboranyl species *via* oxygen–sulphur bond fission [equation (3)]. Evidence for oxygen–sulphur bond scission comes from the analogous reaction between $B_{10}H_{12}(SMe_2)_2$ and *p*-$MeC_6H_4SO_3H$ in which the only products we isolated were $(B_{10}H_{13})_2O$ and di(*p*-tolyl) disulphide, *p*-$MeC_6H_4SSC_6H_4Me$-*p*.

$$B_{10}H_{12}(SMe_2)_2 + HCl \longrightarrow B_{10}H_{13}Cl + 2SMe_2 \quad (1)$$

$$B_{10}H_{12}(SMe_2)_2 + H_2SO_4 \longrightarrow \{B_{10}H_{13}OSO_3H\} + 2SMe_2 \quad (2)$$

$$\{B_{10}H_{13}OSO_3H\} \longrightarrow \{B_{10}H_{13}O-\} + \{-SO_3H\} \quad (3)$$

We believe that both the hydroxide and oxide are produced in the H_2SO_4 reaction rather than as a consequence of the extraction and purification procedure, since we have not observed any significant interconversion between the two species under conditions in which the reaction occurs. Indeed, attempts we have made to interconvert these species using a variety of conditions have so far always been unsuccessful. Thus, treatment of 6-$B_{10}H_{13}OH$ in separate experiments with P_2O_5–C_6H_6, 5% oleum, 98% H_2SO_4, 50% H_2SO_4, or C_6H_6 under reflux (azeotropic dehydration) gave only unchanged 6-$B_{10}H_{13}OH$ and no 6,6′-$(B_{10}H_{13})_2O$. Conversely, treatment of 6,6′-$(B_{10}H_{13})_2O$ with 98% H_2SO_4 gave no hydroxide, and even with 50% H_2SO_4 only a trace of 6-$B_{10}H_{13}OH$ was observed in the bulk of unchanged oxide. Interestingly, however, when a 1:1 mixture of 6-$B_{10}H_{13}OH$ and $B_{10}H_{12}(SMe_2)_2$ was treated with H_2SO_4 (98%) the yield of oxide was increased and that of the hydroxide correspondingly reduced. This may indicate that the probable initial stable product is the hydroxide species, of which the OH group could subsequently react with a second mol of $B_{10}H_{12}(SMe_2)_2$ to generate the oxide in a mode analogous to that believed to occur[14] in the reaction of $B_{10}H_{12}(SMe_2)_2$ with HCl [equation (1)], H_2SO_4 [equation (2)], or $HgCl_2$.

As previously reported,[14] 6,6′-$(B_{10}H_{13})_2O$ proved to be stable to reagents such as Br_2 or PCl_5. However, the hydroxide does react with these reagents: Br_2 produces an insoluble white deposit whereas PCl_5 affords 6-$B_{10}H_{13}Cl$. This difference in reactivity of the two closely related oxo-species may result from the combined effects of the steric protection afforded to the B–O–B linkage by two decaboranyl clusters in the oxide and the relative stabilities of the B–O and O–H bonds.

The non-nucleophilic base *N,N,N′,N′*-tetramethylnaphthalene-1,8-diamine (tmnda) ('proton sponge') reacts readily with both species in neutral dipolar solvents to produce the salt [H-

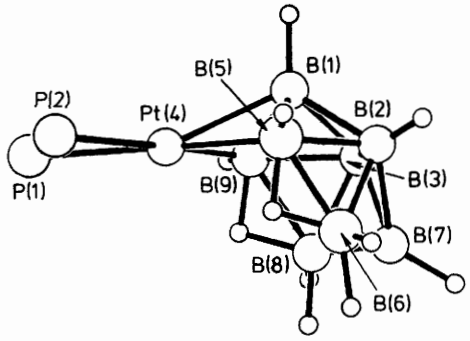

Figure 3. Representation of the molecular structure of [4,4-$(PhMe_2P)_2$-*arachno*-4-PtB_8H_{12}], with P-organo-groups omitted for clarity. In this projection the *exo*-terminal hydrogen atom on B(3) is obscured. The phosphorus atoms P(1) and P(2) are almost exactly *trans* to B(5) and B(9) respectively

tmnda]$^+[B_9H_{14}]^-$ in high yield. This degradation presumably occurs *via* the loss of the B(6) (*i.e.* oxygenated) vertices in both species. This would be consistent with two further considerations. First, the solid-state molecular structure[5] of 6,6′-$(B_{10}H_{13})_2O$ shows the B(6) vertices to be slightly less strongly bonded to the cluster than the corresponding B(9) vertices, and secondly it is reasonable to presume that the relatively inert B–O bond would be unlikely to cleave under the mild conditions used. Although no single-crystal *X*-ray analysis of the hydroxide has been carried out it is likely, on the basis of the n.m.r. spectroscopic data, that the effect of the hydroxyl oxygen upon the decaboranyl cluster is similar to, and probably slightly more pronounced than, that found for the oxide.

It is also of interest to enquire whether the reactions of substituted decaboranes such as the 6-oxy compounds reported here parallel or differ from the reactions that *nido*-decaborane itself undergoes. Decaborane readily forms metallaundecaborane species with a variety of metal halides under general conditions as summarised in equation (4).[15,16]

$$B_{10}H_{14} + [MCl_2L_n] + 2\,\text{base} \longrightarrow [L_nMB_{10}H_{12}] + 2\,[\text{Hbase}]^+Cl^- \quad (4)$$

Accordingly, we have investigated the reactions of $(B_{10}H_{13})_2O$ and $B_{10}H_{13}OH$ with dihalogenobis(phosphine) complexes of platinum, palladium, and nickel, $[MX_2(PR_3)_2]$. The results are to be seen in the context of our general programme of research into the synthesis, structure, and reactivity of metallaborane compounds of the heavier transition metals such as tungsten, rhenium, osmium, iridium, platinum, and gold (*e.g.* refs. 7, 16—38).

2. *Reactions of* $(B_{10}H_{13})_2O$ *and* $B_{10}H_{13}OH$ *with cis*-$[PtCl_2(PMe_2Ph)_2]$ *and Related Platinum Compounds.*—In general the reactions of the oxide and hydroxide with *cis*-$[PtCl_2L_2]$ complexes are very similar. Here we describe the results in terms of the reactions of the oxide, $(B_{10}H_{13})_2O$; differences in detail are to be found in the Experimental section.

The reaction between *cis*-$[PtCl_2(PMe_2Ph)_2]$ and 6,6′-$(B_{10}H_{13})_2O$ in neutral dipolar solvents proceeds smoothly over a period of several hours in the absence of base at ambient temperature. A number of products have been isolated in modest yield. The major product (10.5%) is [4,4-$(PhMe_2P)_2$-*arachno*-4-PtB_8H_{12}] which has been described in detail elsewhere.[22] The compound has an *arachno* nine-vertex skeletal structure (Figure 3) similar to that of *iso*-B_9H_{15}; four electrons from the $Pt(PMe_2Ph)_2$ moiety are thought to be involved in the cluster bonding so the compound may be regarded to a certain extent as a formal platinum(IV) species.

Table 2. Phosphorus-31 n.m.r. data for the unidentified diplatinaborane from the reaction of *cis*-$[PtCl_2(PPh_3)_2]$ and 6,6′-$(B_{10}H_{13})_2O$, with the data for $[(PhMe_2P)_2Pt_2B_8H_{14}]$ included for comparison

	Unidentified diplatinaborane[a]		$[(PMe_2Ph)_2Pt_2B_8H_{14}]$[b]	
	A[c]	B[c]	A[c]	B[c]
$\delta(^{31}P)$/p.p.m.[d]	+44.2	+34.1	+3.8	−1.5
$^1J(^{195}Pt-^{31}P)$/Hz[e]	(+) 3 030	(+) 2 993	(+) 2 990	(+) 2 880
$^2J(^{195}Pt-^{31}P)$/Hz[e]	288	230	250	190
$^3J(^{31}P-^{31}P)$/Hz[f]	95	95	90.5	90.5

[a] In CD_2Cl_2 solution at −70 °C. [b] In $CDCl_3$ solution at −50 °C (ref. 38); structure given in ref. 25. [c] Inequivalent phosphine ligands. [d] ±0.3 p.p.m. [e] ±10 Hz. [f] ±2 Hz.

Detailed considerations indicate that the cluster electronic structure has similarities to a (hypothetical) $[B_9H_{13}]^{2-}$ anion of formal 2532 *styx* topology.[22,36]

A minor product isolated in trace quantities was identified by ^{11}B and ^{31}P n.m.r. spectroscopy as the metallaundecaborane [7,7-$(PhMe_2P)_2$-*nido*-7-$PtB_{10}H_{12}$], again a formal platinum(IV)-type species that has been adequately described elsewhere.[19–21] A third product, in intermediate yield (*ca.* 3.6%), is the interesting and novel 14-vertex *conjuncto*-diplatinatetradecaborane, $[Pt_2(\mu\text{-}\eta^3\text{-}B_6H_9)_2(PMe_2Ph)_2]$, which has been characterised by a single-crystal *X*-ray diffraction study and is discussed in more detail in the next section.

Variation of the reaction by use of *cis*-$[PtCl_2(PPh_3)_2]$ instead of the PMe_2Ph analogue generally resulted in products analogous to those described in the preceding paragraphs, and these were generally identified by comparison of their n.m.r. properties with those of the PMe_2Ph analogues (see Tables 7 and 8 below). Of additional interest was a product with similar chromatographic properties to those of the symmetrical diplatinatetradecaborane $[Pt_2(\mu\text{-}\eta^3\text{-}B_6H_9)_2(PPh_3)_2]$, but for which the ^{31}P n.m.r. properties (Table 2) indicated an asymmetric P_A–Pt_A–Pt_B–P_B system rather than the symmetrical one associated with the symmetrical species. We have not yet been able to isolate this new species, but it may be related to the novel *arachno*-diplatinadecaborane $[(PhMe_2P)_2Pt_2B_8H_{14}]$ which has recently been isolated from another reaction system studied in these laboratories.[25] The ^{31}P n.m.r. properties of this latter species[38a] are also included in Table 2 for comparison.

Finally in this section, it is of interest to note that, when equimolar quantities of 6,6′-$(B_{10}H_{13})_2O$ and *cis*-$[PtCl_2(PMe_2Ph)_2]$ are treated with two mol equivalents of tmnda in methanol rather than CH_2Cl_2 as solvent, then a much more vigorous reaction occurs; $[(PhMe_2P)_2PtB_8H_{12}]$ (78%) and $[Pt_2(\mu\text{-}\eta^3\text{-}B_6H_9)_2(PMe_2Ph)_2]$ (*ca.* 1%) are formed. This reaction can be compared with that of $[B_9H_{14}]^-$ and *cis*-$[PtCl_2(PMe_2Ph)_2]$ in methanol solution (see later).

3. *Molecular Structure and N.M.R. Characterisation of* $[Pt_2(\mu\text{-}\eta^3\text{-}B_6H_9)_2(PMe_2Ph)_2]$.—The compound readily yielded crystals suitable for single-crystal *X*-ray diffraction analysis and a preliminary report has been presented elsewhere.[7] The molecular structure, having crystallographic symmetry C_i, is shown in Figure 4, which also shows the atom numbering. Selected interatomic distances are in Table 3, and angles between interatomic vectors are in Table 4. Hydrogen atoms were not located. However, those on the P-organo-groups are reasonably inferred, and n.m.r. spectroscopy (as summarised in Tables 5 and 6 and in the accompanying text) established the

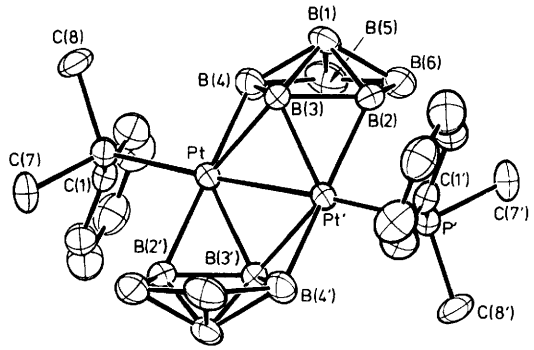

Figure 4. ORTEP drawing of the molecular structure of $[Pt_2(\mu\text{-}\eta^3\text{-}nido\text{-}B_6H_9)_2(PMe_2Ph)_2]$. Hydrogen atoms were not located in the diffraction analysis, but n.m.r. spectroscopy shows that each boron atom has an *exo*-terminal hydrogen bound to it, and that there are bridging hydrogen atoms at borane cluster sites (2,6), (4,5), and (5,6) (see Table 5). Peaks corresponding to these positions appeared in final difference maps (see Experimental section)

Table 3. Interatomic distances (pm) for $[Pt_2(\mu\text{-}\eta^3\text{-}B_6H_9)_2(PMe_2Ph)_2]$ with estimated standard deviations in parentheses

(*a*) From the platinum atoms			
Pt(1)–Pt(1′)	264.4(1)	Pt(1)–B(3)	217.8(7)
Pt(1)–P(1)	230.2(2)	Pt(1′)–B(4)	222.8(10)
Pt(1)–B(2)	222.2(10)	Pt(1′)–B(3)	222.4(9)
(*b*) Boron–boron			
B(1)–B(2)	179.9(14)	B(2)–B(3)	180.4(12)
B(1)–B(3)	182.2(13)	B(2)–B(6)	180.9(16)
B(1)–B(4)	179.8(13)	B(3)–B(4)	182.5(14)
B(1)–B(5)	176.5(14)	B(4)–B(5)	178.0(15)
B(1)–B(6)	175.7(15)	B(5)–B(6)	174.7(16)
(*c*) Phosphorus–carbon		(*d*) Other	
P(1)–C(1)	181.9(8)	C–C(Ph)	136.1—139.2(14)
P(1)–C(7)	183.2(9)		(mean 138.3)
P(1)–C(8)	182.0(8)		

following: (*i*) each boron atom has one terminal hydrogen atom associated with it; (*ii*) there is a bridging hydrogen atom between each of the equivalent B(2)B(6) and B(4)B(5) atom pairs of each sub-cluster, and (*iii*) there is a unique bridging hydrogen atom between the B(5) and B(6) atoms of each six-boron sub-cluster.

The structure (Figure 4) has an essentially linear P–Pt–Pt′–P′ system (P–Pt–Pt′ = 175.5°) with two *nido*-type six-vertex 2,3,4-η^3-B_6H_9 ligands symmetrically bonded to the metal atoms. Interatomic distances and angles within each six-boron sub-cluster are within normal ranges and the compound may be viewed in the first instance (see below) as a complex between two bidentate *nido*-$[\eta^3\text{-}B_6H_9]^-$ anionic ligands and $[(PMe_2Ph)Pt\text{–}Pt(PMe_2Ph)]^{2+}$. The parent *nido*-borane B_6H_{10} is generally regarded as having a basal B–B bond (**VII**) which is sufficiently basic to act as a ligand to platinum, *e.g.* in $[PtCl_2(B_6H_{10})_2]$.[39,40] Its formal deprotonation would result in two such basic sites, (**VIII**) or (**IX**). If these are adjacent, (**VIII**), they may in principle [although see discussion below structure (**XV**)], act as a trihapto bidentate ligand as in $[Pt_2(\mu\text{-}\eta^3\text{-}B_6H_9)_2(PMe_2Ph)_2]$ described here [structure (**X**)]. Alternatively when they are non-adjacent, as in (**IX**), then a bis(monodentate) bis(dihapto) bonding mode may be adopted,* as is believed to occur in $[Ti_2(B_6H_9)_2(C_5H_5)_4]$ and related species.[16,41]

Table 4. Angles (°) between interatomic vectors for $[Pt_2(\mu\text{-}\eta^3\text{-}B_6H_9)_2(PMe_2Ph)_2]$ with estimated standard deviations in parentheses

(*a*) At the platinum atoms			
Pt′–Pt–P	175.5(1)	Pt–B(3)–Pt′	73.8(3)
Pt–Pt′–B(2)	94.6(3)	Pt′–Pt–B(4)	91.7(3)
Pt–Pt′–B(3)	53.9(2)	Pt′–Pt–B(3)	52.3(2)
P′–Pt′–B(2)	86.8(3)	P–Pt–B(4)	87.6(3)
P′–Pt′–B(3)	123.0(2)	P–Pt–B(3)	130.6(2)
B(2)–Pt′–B(3′)	141.4(4)	B(4)–Pt–B(3′)	132.8(3)
B(2)–Pt–B(3)	47.9(3)	B(4)–Pt–B(3)	48.9(4)
B(2)–Pt′–B(4′)	168.9(4)	B(3)–Pt–B(3′)	106.2(3)
(*b*) Platinum–boron–boron			
Pt′–B(2)–B(1)	120.8(5)	Pt–B(4)–B(1)	121.9(5)
Pt′–B(2)–B(3)	66.1(5)	Pt–B(4)–B(3)	64.1(5)
Pt′–B(2)–B(6)	122.0(5)	Pt–B(4)–B(5)	128.4(6)
Pt′–B(3)–B(1)	119.6(5)	Pt–B(3)–B(1)	123.4(5)
Pt′–B(3)–B(4)	119.8(5)	Pt–B(3)–B(2)	128.3(5)
Pt′–B(3)–B(2)	66.0(5)	Pt–B(3)–B(4)	67.0(5)
(*c*) Boron–boron–boron		(*d*) Platinum–phosphorus–carbon	
Range 57.3—62.1, mean 60.0		Pt–P–C(1)	112.6(3)
Range 107.3—110.1, mean 108.6		Pt–P–C(7)	119.6(3)
		Pt–P–C(8)	116.3(3)

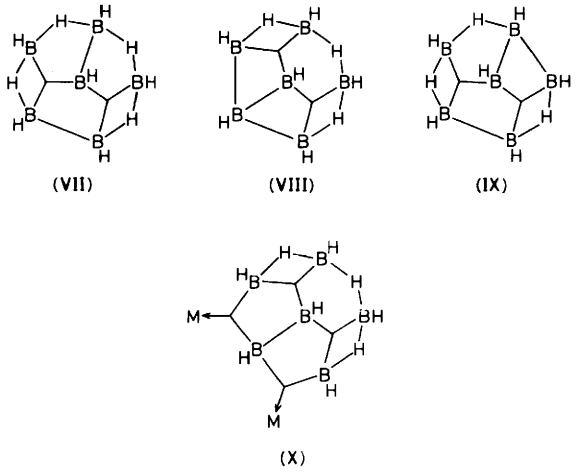

The platinum–platinum bond length of 264.4 pm is comparable with similar lengths in compounds such as $[Pt_2(\mu\text{-}\eta^3\text{-}C_4H_7)(\mu\text{-}\eta^3\text{-}C_5H_5)(PPr^i_3)_2]$, $[Pt_2(\mu\text{-}\eta^2\text{-}SPMe_2)_2\{P(OMe)_3\}_2]$, and $[\{Pt(CNMe_3)_3\}_2]$, and in the closely related compound $[Pt_2(\mu\text{-}\eta^3\text{-}B_6H_9)(\mu\text{-}B_2H_5)(PMe_2Ph)_2]$.[35,38a,42]

The appropriate elements of the structure bear some similarities to allyl–metal–metal bonding in such compounds as $[Pd_2(\mu\text{-}\eta^3\text{-}C_3H_4Me)_2(PPr^i_3)_2]$ where both allyl ligands are believed to be disposed about the palladium atoms in a manner similar to that found by *X*-ray diffraction analysis of the related $[Pd_2(\mu\text{-}\eta^3\text{-}C_5H_5)(\mu\text{-}\eta^3\text{-}C_3H_4Me)(PPh_3)_2]$: the platinum analogue of this latter compound is known, but not that of the former.[43,44]

The overall structure also bears a geometrical relationship to the known binary neutral boron hydride $B_{14}H_{20}$ [structure

* Throughout we use 'denticity' to indicate the presumed number of two-electron bonds formed by donation to the metal centres, and 'hapticity' to indicate the connectivity of the borane clusters to the metal centres.

Table 5. Boron-11 and associated proton n.m.r. data for $[Pt_2(\mu\text{-}\eta^3\text{-}B_6H_9)_2(PMe_2Ph)_2]$; saturated $CDCl_3$ solution at +21 °C

Assignment[a]	1	2,4	3	5,6	Bridge	
$\delta(^{11}B)$/p.p.m.	−42.0	−3.6	+59.7	+8.3		
$^1J(^{11}B\text{–}^1H)$/Hz	140 ± 5	135 ± 10	135 ± 10	130 ± 10		
Approx. $T_1(^{11}B)$/ms[b]	7.7	*ca.* 0.9	2.5	*ca.* 1.0		
$^1J(^{195}Pt\text{–}^{11}B)$/Hz	—	300 ± 20	330 ± 20[c]	—		
Relative intensity	1	2	1	2		
$\delta(^1H)$/p.p.m.	+0.72	+3.13	+6.00	+4.13	−1.01	−1.14
Relative intensity	1	2	1	2	2	1
$^nJ(^{195}Pt\text{–}^1H)$/Hz	41 ± 4	79 ± 5	38 ± 3	—	52 ± 5	—
$\Delta\sigma(^{11}B)$/p.p.m.[d]	−9.8	+17.7	−45.6	+5.8	—	—

[a] See text; based principally on relative intensities and the incidence of coupling $^1J(^{195}Pt\text{–}^{11}B)$. [b] Saturated $CDCl_3$ solution at *ca.* 21 °C, ±0.5 ms. [c] Satellites apparent for species with both one and two ^{195}Pt nuclei per molecule. [d] $\Delta\sigma$ = substituent shielding effect = $\delta(B_6H_{10})$ − $\delta[Pt_2(\mu\text{-}\eta^3\text{-}B_6H_9)_2(PMe_2Ph)_2]$, and is the increase in *shielding* over the unsubstituted B_6H_{10} (see Table 1, footnote *c*).

Table 6. Phosphorus-31 and associated proton n.m.r. data for $[Pt_2(\mu\text{-}\eta^3\text{-}B_6H_9)_2(PMe_2Ph)_2]$

(*a*) Phosphorus-31		
Temp. (°C)[a]	−52	−91
$^1J(^{195}Pt\text{–}^{31}P)$/Hz[b]	+2 817 ± 5	+2 812 ± 5
$^2J(^{195}Pt\text{–}^{31}P)$/Hz[b]	+288 ± 3	+283 ± 3
$^3J(^{31}P\text{–}^{31}P)$/Hz	97 ± 2	96 ± 2
$\delta(^{31}P)$/p.p.m.	−0.03	+0.75
(*b*) Proton		
P-methyl groups[c]	A	B
$\delta(^1H)$/p.p.m.	+2.11	+2.55
$^3J(^{195}Pt\text{–}^1H)$/Hz[d]	+28.8	+27.8
$^2J(^{31}P\text{–}^1H)$/Hz[d]	(−)9.2	(−)9.5
Relative intensity	1	1

[a] In saturated CD_2Cl_2 solution at low temperatures to maximise 'thermal decoupling' of boron nuclei (ref. 18). [b] The position of the '*N*' lines (see text and ref. 51) indicates these couplings are of the same sign (both presumably positive as indicated). [c] Saturated $CDCl_3$ solution at *ca.* 21 °C; A and B distinguish the two chemically inequivalent methyl group resonances. [d] Proton coupling constants ±0.5 Hz.

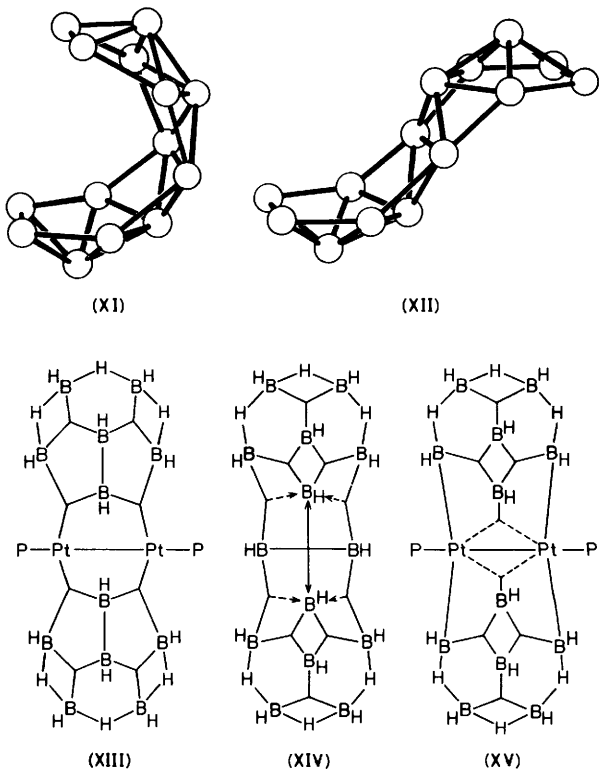

(**XI**)] of C_{2v} symmetry,[45] the diplatinum compound being isostructural with the (hypothetical) isomer with C_2 symmetry [structure (**XII**)]; this may perhaps suggest that this isomer could be synthesised as a stable *conjuncto*-borane, though by what route is not at present clear. Also, conversely, it should be pointed out that we have not detected an isomer of $[Pt_2(\mu\text{-}\eta^3\text{-}B_6H_9)_2(PMe_2Ph)_2]$ that would correspond to structure (**XI**) in our reaction products. It cannot be decided on present evidence whether this is due to kinetic effects, or whether the different orbital-geometry requirements of the $(PhMe_2P)Pt$ and BH fragments will preclude the complementary structure in each case.[24] Certainly the isolated compound is very stable and, subsequent to its initial characterisation, we have detected it as a degradation product, sometimes in substantial quantities, in a number of reactions involving phosphine platinum species with eight-, nine-, and ten-vertex boron hydride derivatives.[22,24,25,38]

In view of this stability, the electronic structure of $[Pt_2(\mu\text{-}\eta^3\text{-}B_6H_9)_2(PMe_2Ph)_2]$ merits some discussion, as the straightforward rationale based on bis(bidentate) hexaboranyl ligands (**VIII**) with major contributions from canonical forms such as structures (**X**) and (**XIII**) is undoubtedly oversimplified.[25] Although the formal binary borane analogue $B_{14}H_{20}$ has a formal $2n + 6$ and therefore *arachno* electron count, this type of terminology has a limited meaning in macropolyhedral *conjuncto* species, and the $B_{14}H_{20}$ molecule, although symmetrical, is better viewed as a cluster species derived from an *arachno*-B_8H_{14} cluster sharing a diboron common edge with a *nido*-B_8H_{12} cluster. Of these, *nido*-B_8H_{12} has an anomalous unsaturated *arachno*-type geometry,[46,47] and is readily stabilised by the acceptance of an electron pair.[48] In the *conjuncto arachno–nido* species $B_{14}H_{20}$ this electron deficiency can be regarded as being distributed symmetrically between the two eight-vertex sub-clusters, and is believed to be alleviated somewhat by the diversion of electron density from the B(7)–B(12) bond towards the B(2) and B(3) atoms to give a bond of four-centre character as in structure (**XIV**).[49] In the diplatinum species this role is in principle more readily fulfilled by electron-pair donation *via* filled metal *dp* hybrid orbitals of appropriate symmetry which will presumably be available in this soft bonding environment, and it is therefore probable that the electronic structure about the platinum atoms contains

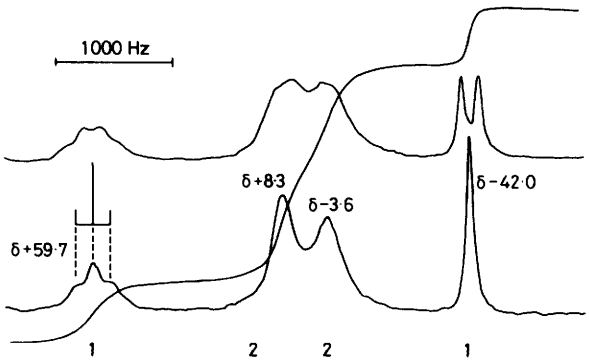

Figure 5. 32-MHz ^{11}B (top trace) and ^{11}B-{^{1}H(broad band noise)} (bottom trace) n.m.r. spectra of $[Pt_2(\mu\text{-}\eta^3\text{-}B_6H_9)_2(PMe_2Ph)_2]$ in CD_2Cl_2 solution at +21 °C; $\delta(^{11}B)$ in p.p.m. to low field of $Et_2O\cdot BF_3$. The B(3) resonance at $\delta(^{11}B)$ +59.7 p.p.m. exhibits satellites arising from coupling $^{1}J(^{195}Pt\text{–}^{11}B)$: dashed lines indicate the lines arising from species with no ^{195}Pt nucleus in the molecule (*ca.* 54%) and one ^{195}Pt in the molecule (*ca.* 33%). Additional satellite intensity arises from those molecules containing two ^{195}Pt nuclei (*ca.* 11%)

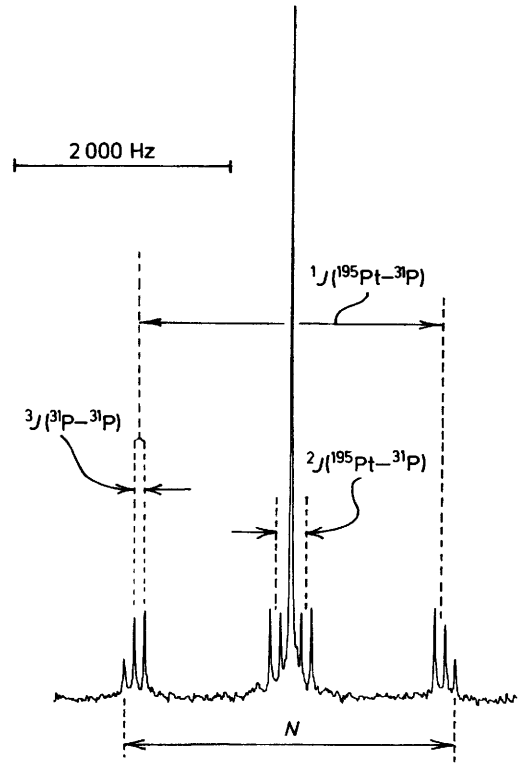

Figure 6. 40.25-MHz ^{31}P-{^{1}H(broad band noise)} n.m.r. spectrum of $[Pt_2(\mu\text{-}\eta^3\text{-}B_6H_9)_2(PMe_2Ph)_2]$ in CD_2Cl_2 solution at −51 °C. The lines with separation N arise from molecules containing two ^{195}Pt nuclei, and $N = {}^{1}J(^{195}Pt\text{–}^{31}P) + {}^{2}J(^{195}Pt\text{–}^{31}P)$ (see text and ref. 51)

significant contributions from canonical forms such as (**XV**). In these last, the metal centres can be regarded as each contributing four electrons to the cluster bonding and may thus be ascribed the valency state of IV; platinum(IV)-type contributions of this nature seem often to be involved when platinum is found in a contiguous polyhedral metallaborane cluster.[21,26] This formulation implies a significant deviation from $[B_6H_9]^-$ character for the central boron atom in the trihapto system, which may well be related to the anomalously low nuclear shielding of this atom. By contrast, straightforward dihapto donation to platinum(II) is known to perturb the nuclear shielding of the boron atoms involved by only a few p.p.m.[13,17,18,38]

The interpretation of the ^{11}B, ^{1}H, and ^{31}P n.m.r. parameters for the compound are in fact straightforward. Boron-11 and borane ^{1}H data are summarised in Table 5, and phosphine proton and ^{31}P data in Table 6. Boron-11 nuclei were related to their directly bonded terminal hydrogen atoms by selective ^{1}H-{^{11}B} spectroscopy,[4,13,19,22] which was also used to determine the relative signs[19] of $^{1}J(^{195}Pt\text{–}^{11}B)$ and $^{2}J(^{195}Pt\text{–}^{1}H)$ where stated in the Tables. The 1:2:2:1 intensity pattern in the ^{11}B spectrum (Figure 5) together with the incidence of $^{1}J(^{195}Pt\text{–}^{11}B)$ = *ca.* 300 Hz readily assigns the boron resonances (and their terminal hydrogen atom resonances) and the assignment of the bridging protons follows from their 2:1 intensity ratio. The boron and proton chemical shifts and coupling constants in general are not anomalous and follow previously established patterns,[13,17-22] the exception being the low-field resonance for B(3) which may perhaps be diagnostic of the electronic contributions from two flanking metal atoms in this type of system as discussed above. An additional factor worth mentioning is that if the structural analogy with $B_{14}H_{20}$ is admissable, and if the subrogation of BH by $Pt(PMe_2Ph)$ mainly affects those atoms nearest to the subrogation centre, then this may necessitate a partial revision of the proposed ^{11}B assignments for $B_{14}H_{20}$;[45,50] however, these initial assignments for $B_{14}H_{20}$ were understandably at best tentative. It would obviously be very useful to have two-dimensional n.m.r. boron–boron correlation spectroscopy performed on this and the other Schaeffer macropolyhedral binary boranes.

The ^{31}P n.m.r. spectrum is of some interest since, in addition to the singlet resonance arising from those molecules which do not contain ^{195}Pt (34% natural abundance), there are also resonance lines arising from species containing one and two ^{195}Pt atoms (Figure 6 and Table 6). The two AMX-type sub-sub-spectra arising from the $^{31}P\text{–}^{195}Pt\text{–}Pt\text{–}^{31}P$ system are readily visible and interpretable, and the ^{31}P '*N*' lines from the $[AX]_2$ system[51] arising from the $^{31}P\text{–}^{195}Pt\text{–}^{195}Pt\text{–}^{31}P$ isotopic combination are also readily seen, their positions indicating that $^{2}J(^{195}Pt\text{–}^{31}P)$ and $^{1}J(^{195}Pt\text{–}^{31}P)$ have the same sign and are therefore both presumably positive. The other ^{31}P lines[51] of this $[AX]_2$ system, however, were not apparent under experimental conditions which would have revealed them if $^{1}J(^{195}Pt\text{–}^{195}Pt)$ were of small or intermediate magnitude; this implies that this coupling constant is large (*i.e.* a few thousand Hz). This would result in the outer lines being undetectably small and the inner lines being essentially coincident with the central resonance agglomerate at $\nu(^{31}P)$, the coincidence precluding an estimation of J *via* the $(L^2 - S^2)/2S$ formula. This large (and presumably positive) coupling constant is consistent with the postulated direct platinum–platinum bond, since bridged Pt_2 systems with no direct intermetallic bond have much smaller couplings which may even take a negative sign. For example, ^{31}P-{^{1}H,^{195}Pt} selective triple-resonance spectroscopy shows that $^{2}J(^{195}Pt\text{–}^{195}Pt)$ is −205 Hz for the chloro-bridged dimer $[Pt_2Cl_4(PBu^n_3)_2]$.[52]

The P-methyl proton n.m.r. parameters merit little comment except to note that the platinum atoms are prochiral centres; consequently the Pt–P vector is not contained in a molecular mirror symmetry plane and the two phosphine P-methyl groups are therefore chemically inequivalent and exhibit separate n.m.r. resonance patterns which will have features associable with $[AX_3Y_3]_2$-type spin systems.[21]

The ^{11}B, ^{1}H, and ^{31}P n.m.r. data for the triphenylphosphine species $[Pt_2(\mu\text{-}\eta^3\text{-}B_6H_9)_2(PPh_3)_2]$ {and also $[(Ph_3P)_2PtB_8H_{12}]$} are summarised in Tables 7 and 8 respectively and exhibit no unusual features when compared to the PMe_2Ph analogues.

Table 7. Boron-11,[a] proton,[a] and phosphorus-31[b] n.m.r. data for $[Pt_2(\mu\text{-}\eta^3\text{-}B_6H_9)_2(PPh_3)_2]$ in $CDCl_3$ solution

Assignment[c]	1	2,4	3	5,6	Bridge	
$\delta(^{11}B)$/p.p.m.	−42.3	−1.4	+60.5	+5.5		
$\Delta\sigma(^{11}B)$/p.p.m.[d]	−9.5	+15.5	−46.4	+8.6		
$^1J(^{11}B\text{–}^1H)$/Hz	142 ± 10	*e*	*e*	*e*		
Relative intensity	1	2	1	2		
$\delta(^1H)$/p.p.m.	+0.87	+3.10	+6.75	+3.94	−1.15	−1.03
$^nJ(^{195}Pt\text{–}H)$/Hz	50 ± 10	38 ± 10	40 ± 5	*f*	*f*	60 ± 10
Relative intensity	1	2	1	2	1	2
$\delta(^{31}P)$/p.p.m.	+39.0					
$^1J(^{195}Pt\text{–}^{31}P)$/Hz	+2 866 ± 5					
$^2J(^{195}Pt\text{–}^{31}P)$/Hz	+328 ± 3					
$^3J(^{31}P\text{–}^{31}P)$/Hz	103 ± 3					

[a] Recorded at +21 °C. [b] Recorded at −50 °C. [c] Assignment based upon $[Pt_2(\mu\text{-}\eta^3\text{-}B_6H_9)_2(PMe_2Ph)_2]$, see text and Table 5. [d] $\Delta\sigma$ = substituent shielding effect = $\delta(^{11}B)(B_6H_{10}) - \delta(^{11}B)[Pt_2(\mu\text{-}\eta^3\text{-}B_6H_9)_2(PPh_3)_2]$ (see Table 1, footnote *c*). [e] Not measurable due to broad and/or overlapping resonances. [f] Not observed.

Table 8. Boron-11,[a] proton,[a] and phosphorus-31[b] n.m.r. data for $[4,4\text{-}(Ph_3P)_2\text{-}4\text{-}PtB_8H_{12}]$ in $CDCl_3$ solution

Assignment[c]	1	7	9,5	6,8	2,3	Bridge (5,6) and (8,9)	*endo*-Terminal (6) and (8)
$\delta(^{11}B)$/p.p.m.	+22.0	+18.0	+2.0	−24.4	−30.6		
Relative intensity	1	1	2	2	2		
$\Delta\sigma(^{11}B)$/p.p.m.[d]	+2.9	+6.9	−19.3	+3.7	−7.6		
$^1J(^{11}B\text{–}^1H)$/Hz	*e*	*e*	*e*	*e*	138 ± 20		
$\delta(^1H)$/p.p.m.	+4.32	+4.07	+2.70	+1.64	+0.87	−3.10	+0.21
Relative intensity	1	1	2	2	2	2	2
$\delta(^{31}P)$/p.p.m.	+27.3 ± 0.5						
$^1J(^{195}Pt\text{–}^{31}P)$/Hz	+2 822 ± 5						

[a] Recorded at 21 °C. [b] Recorded at −50 °C. [c] Assignment based upon $[(PhMe_2P)_2PtB_8H_{12}]$ (ref. 22). [d] $\Delta\sigma$ = substituent shielding effect = $\delta(^{11}B)(B_8H_{14}) - \delta(^{11}B)[(Ph_3P)_2PtB_8H_{12}]$ (see Table 1, footnote *c*). [e] Not measurable due to broad and/or overlapping resonances.

Table 9. Selected boron-11, proton, and phosphorus-31 n.m.r. data for $PhMe_2P\cdot B_9H_{13}$;[a] $CDCl_3$ solution at +21 °C

Assignment[b]	1	2,3	4	5,9	6,8	7	Bridge (5,6) and (8,9)
$\delta(^{11}B)$/p.p.m.	+3.36	−38.5	−36.3[c]	−15.1	−21.8	+18.4	
Relative intensity	1	2	1	2	2	1	
Approx. $T_1(^{11}B)$/ms	8.2	18.0	13.0	8.5	4.0	1.9	
$^1J(^{11}B\text{–}^1H)$/Hz	135 ± 5	145 ± 5	*d*	145 ± 5	140 ± 10	160 ± 10	
$\delta(^1H)$/p.p.m.[e]	+3.14	+0.75	−0.18[f,g]	+2.10	+2.12,[h] +0.29[g]	+4.36	−3.09
Relative intensity	1	2	1	2	2	1	2

[a] $\delta(^{31}P)$ = −1.8 p.p.m. [b] Assignment based upon published data for $Ph_3P\cdot B_9H_{13}$ (ref. 55). [c] Doublet, $^1J(^{31}P\text{–}^{11}B)$ = 120 ± 5 Hz. [d] Not measured. [e] Assigned by $^1H\text{-}\{^{11}B(\text{selective})\}$ experiments. [f] Doublet, $^2J(^{31}P\text{–}^1H)$ = 9.8 ± 0.5 Hz. [g] *endo*-Hydrogen atoms. [h] *exo*-Hydrogen atom.

4. *Reactions of* $(B_{10}H_{13})_2O$ *with Dihalogenobis(phosphine) Complexes of Nickel*(II) *and Palladium*(II).—The reaction of $(B_{10}H_{13})_2O$ with *cis*-$[NiCl_2(PMe_2Ph)_2]$ under similar conditions to those of the corresponding platinum reaction described above (section 2) resulted in only a small yield of an isolable and identifiable metallaborane species. The principal products isolated included the phosphine–borane adducts $PhMe_2P\cdot BH_3$ (33.7%) and $PhMe_2P\cdot B_3H_7$ (8.8%) (of the type which have already been described in the literature) [53,54] together with the larger *arachno* nine-vertex cluster $PhMe_2P\cdot B_9H_{13}$ (28%). Ligand–B_9H_{13} adducts are well known,[55,56] but a number of their n.m.r. properties, particularly those of ^1H, are not thoroughly established, and so we report the ^1H and ^{11}B properties here (Table 9). Some aspects of the shielding behaviour of this and other species are discussed below in section 7.

The only stable metallaborane that we have been able to isolate from this particular reaction is the interesting red *closo* ten-vertex 1-nickeladecaborane, $[(PhMe_2P)_2NiB_9H_7Cl_2]$, which was characterised by single-crystal *X*-ray diffraction analysis as

Table 10. Boron-11 n.m.r. data for the metallaborane complex thought to be $[(dppe)NiB_8H_{12}]$, in $CDCl_3$ solution at +21 °C

Assignment[a]	1	7	5,9	6,8	2,3
$\delta(^{11}B)$/p.p.m.[b]	+16	+14	+2	−18	−32
$\triangle\sigma(^{11}B)$/p.p.m.[c]	+8.9	+10.6	−22.7	−2.7	−6.2
Relative intensity	1	1	2	2	2
$^1J(^{11}B-^1H)$/Hz	*d*	*d*	120 ± 20	120 ± 20	130 ± 20

[a] Assignment based upon the previously described spectra for $[(PhMe_2P)_2PtB_8H_{12}]$ (ref. 22). [b] ±2 p.p.m. due to broad overlapping resonances. [c] $\triangle\sigma$ = substituent shielding effect = $\delta(^{11}B)(B_8H_{14}) - \delta(^{11}B)[(dppe)NiB_8H_{12}]$ (see Table 1, footnote *c*). [d] Not measured due to overlapping resonances.

Table 11. Boron-11,[a] proton,[a] and phosphorus-31[b] n.m.r. data for $[(PhMe_2P)_2PdB_8H_{12}]$ in CD_2Cl_2 solution

Assignment[c]	1	7	5,9	6,8	2,3	Bridge (5,6) and (8,9)	*endo*-Terminal (6) and (8)
$\delta(^{11}B)$/p.p.m.	+22.5	+15.4	+5.5	−22.3	−29.4		
$\triangle\sigma(^{11}B)$/p.p.m.[d]	+2.4	+9.5	−26.2	+1.7	−8.8		
Relative intensity	1	1	2	2	2		
$^1J(^{11}B-^1H)$/Hz	120 ±20	*e*	120 ±20	120 ±20	145 ±10		
$\delta(^1H)$/p.p.m.[f]	+4.08	+4.08	+3.06	+2.17	+0.84	−2.49	+0.71
Relative intensity	1	1	2	2	2	2	2
$\delta(^{31}P)$/p.p.m.		−11.6					
$\delta(^1H)$(MeP)/p.p.m.[g]		+1.54(A)	+1.45(B)				
$[^2J(^{31}P-^1H) +$ $^4J(^{31}P-^1H)]$(MeP)/Hz[g]		7.6 ± 5(A)	7.2 ± 5(B)				

[a] Measured at +21 °C. [b] Measured at −42 °C. [c] Assignment based upon the previously discussed spectra of $[(PhMe_2P)_2PtB_8H_{12}]$ (ref. 22). [d] $\triangle\sigma$ = substituent shielding effect = $\delta(^{11}B)(B_8H_{14}) - \delta(^{11}B)[(PhMe_2P)_2PdB_8H_{12}]$ (see Table 1, footnote *c*). [e] Not measured. [f] Assigned by $^1H-\{^{11}B(selective)\}$ experiments. [g] Two inequivalent P-methyl groups A and B.

Table 12. Boron-11 n.m.r. data for $[(Ph_3P)_2PdB_8H_{12}]$ in $CDCl_3$ solution at +21 °C

Assignment[a]	1	7	5,9	6,8	2,3
$\delta(^{11}B)$/p.p.m.	+21.3	*ca.* +16	+4.0	−22.9	−28.1
Relative intensity	1	1	2	2	2
$\triangle\sigma(^{11}B)$/p.p.m.[b]	+3.6	*ca.* +9	−24.7	+2.2	−10.1
$^1J(^{11}B-^1H)$/Hz	110 ± 20	*c*	*c*	130 ± 20	160 ± 10

[a] Assignment based upon the previously described $[(PhMe_2P)_2PtB_8H_{12}]$ (ref. 22). [b] $\triangle\sigma$ = substituent shielding effect = $\delta(^{11}B)(B_8H_{14}) - \delta(^{11}B)[(Ph_3P)_2PdB_8H_{12}]$ (see Table 1, footnote *c*). [c] Not measured due to broad and/or overlapping resonances.

described in section 5 below. However, this red solid was only present in trace amounts (< 1%).

The course of the reaction, which produces principally phosphine–borane species, may well be influenced by the relative lability of the *cis*-$[NiCl_2(PMe_2Ph)_2]$ complex compared to that of the platinum analogue; this would result in preferential attack by free phosphine on the borane clusters as opposed to metallaborane formation. Somewhat consistent with this, the complex of nickel chloride and the chelating ligand $Ph_2PCH_2CH_2PPh_2$ (dppe), when allowed to react with $[NMe_4][B_9H_{14}]$, produces a metallaborane species tentatively identified by n.m.r. spectroscopy as $[(dppe)NiB_8H_{12}]$, *i.e.* the Ni(dppe) analogue of the compound [7,7-$(PhMe_2P)_2$-*arachno*-7-PtB_8H_{12}] mentioned above (*e.g.*, Figure 3); however, the product seems relatively unstable and the characterisation based upon ^{11}B n.m.r. spectroscopy (Table 10) remains tentative.

The reactions of the palladium complexes *cis*-$[PdCl_2L_2]$ (L = PMe_2Ph or PPh_3) with $(B_{10}H_{13})_2O$, as may perhaps be expected, result in behaviour intermediate between that exhibited by the platinum and nickel species described above. Thus, although significant quantities of the phosphine–borane adducts $L{\cdot}BH_3$, $L{\cdot}B_3H_7$, and $L{\cdot}B_9H_{13}$ were formed,[53–55] isolable metallaborane species were also present, in particular the *arachno* palladanonaboranes, $[(PhMe_2P)_2PdB_8H_{12}]$ and $[(Ph_3P)_2PdB_8H_{12}]$, identified as such by n.m.r. spectroscopy and comparison with the platinum analogue (Tables 11 and 12). A number of other products were present, but these appeared to be much less stable than the $[L_2PdB_8H_{12}]$ species, and their separation in pure form was precluded by decomposition under the separatory conditions so far employed. From the $^{11}B-\{^1H\}$ n.m.r. spectra of these species, several appeared to be metallaboranes, and one in particular exhibited resonance shapes and chemical shifts which encouraged the belief that it might be the palladium analogue of $[Pt_2(\mu\text{-}\eta^3\text{-}B_6H_9)_2(PMe_2Ph)_2]$ (section 3 above) but this conclusion is necessarily tentative.

5. *Characterisation and Structure of* [1,1-$(PhMe_2P)_2$-2,4-Cl_2-*closo*-1-NiB_9H_7].—A few red crystals were isolated from the above reaction between *cis*-$[NiCl_2(PMe_2Ph)_2]$ and 6,6′-$(B_{10}H_{13})_2O$; and one of these was suitable for single-crystal *X*-ray diffraction analysis. The crystals were monoclinic, space

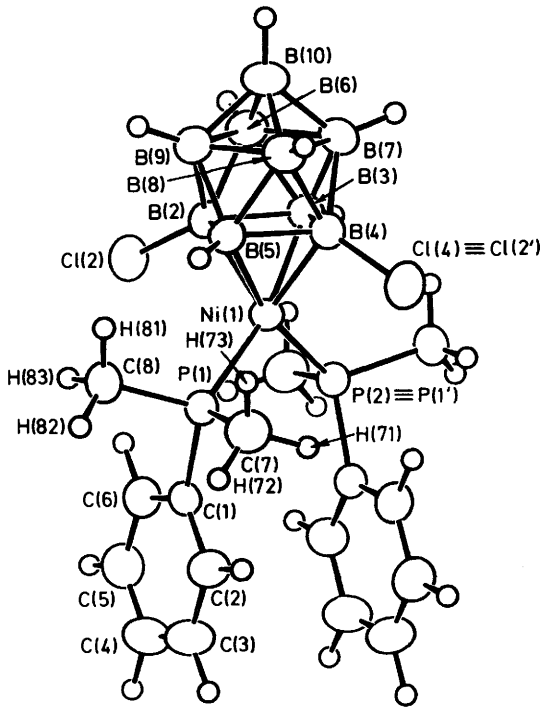

Figure 7. ORTEP drawing of the molecular structure of [1,1-$(PhMe_2P)_2$-2,4-Cl_2-*closo*-1-NiB_9H_7]. The molecule has crystallographic C_2 symmetry; B(4) ≡ B(2′), B(5) ≡ B(3′), B(7) ≡ B(9′), and B(8) ≡ B(6′). Selected molecular dimensions are given in Tables 13 and 14. For crystallographic reasons the numbering system is the enantiomer of the I.U.P.A.C. recommended[8] one [structure (II)]

group $C2/c$ and the molecule, which has crystallographic symmetry C_2, is shown in Figure 7. Selected interatomic distances are given in Table 13 and angles between interatomic vectors are given in Table 14. Hydrogen atoms were located and the cluster was thereby found to have seven terminal BH units and no bridging hydrogen atoms.

The molecular structure of this compound (Figure 7) is based on a *closo* deltahedral ten-vertex NiB_9 cluster which takes the form of a bicapped Archimedian square antiprism with the metal atom occupying one of the two four-connected capping positions. A similar metal connectivity also occurs in some other similar species.[16,57,58] The two chlorine substituents are attached to *trans* (non-adjacent) boron atoms in the B_4 'open face' of the nine-vertex *iso-nido*-type $B_9H_7Cl_2$ fragment, and thus occupy geminal positions relative to the metal centre. Interestingly, the bicapped square antiprismatic geometry, although common in metallacarbaborane chemistry (*e.g.* ref. 35), is not yet well established in metallaborane chemistry. The other known structurally characterised *closo*-MB_9 ten-vertex species take the *iso-closo* geometry of three-fold symmetry.[16,34,37b]

The boron–boron interatomic distances are typical for *closo*-polyhedral boranes and only those associated with the four-atom metal–boron interface deviate noticably (by *ca.* 6 pm) from the corresponding distances[59] in $[B_{10}H_{10}]^{2-}$. The nickel–boron interatomic distances are also typical.[57,58]

The *closo*-geometry (*cf.* $[B_{10}H_{10}]^{2-}$)[59] indicates that the Ni-$(PMe_2Ph)_2$ moiety may to some extent be regarded as a $[BH]^{2-}$-type subrogator, *i.e.* the nickel atom is contributing four electrons to the NiB_9 skeletal bonding and is therefore formally a nickel(IV) species. The tetrahapto borane-to-metal bonding is also known in the related metallacarbaborane chemistry, for example in *closo*-[1,1-$(Me_3P)_2$-6,8,1-$C_2PtB_6H_8$][60] and in *closo*-[4,5-Me_2-6,6-L_2-4,5,6-$C_2NiB_6H_6$] (L = PMe_3 or PEt_3).[61]

Table 13. Selected interatomic distances (pm) for [1,1-$(PhMe_2P)_2$-2,4-Cl_2-*closo*-1-NiB_9H_7] with estimated standard deviations in parentheses *

(*a*) From the nickel atom		(*b*) Boron–boron	
Ni(1)–P	225.8(1)	B(2)–B(3)	182.1(4)
Ni(1)–B(2)	201.0(3)	B(2)–B(6)	178.3(5)
Ni(1)–B(3)	209.3(3)	B(3)–B(6)	178.0(5)
		B(6)–B(7)*	183.5(5)
(*c*) Boron–chlorine and boron–hydrogen		B(6)–B(9)	187.4(6)
B(2)–Cl	179.9(3)	B(6)–B(10)	170.8(5)
B(3)–H(3)	106(4)	B(2)–B(5)*	180.4(6)
B(6)–H(6)	112(4)	B(2)–B(9)	179.5(5)
B(9)–H(9)	106(4)	B(5)*–B(9)	177.1(5)
B(10)–H(10)	108(5)	B(9)–B(10)	171.1(5)
(*d*) Phosphorus–carbon			
P–C(1)	181.3(2)		
P–C(7)	181.9(4)		
P–C(8)	181.8(3)		

* The molecule has crystallographic C_2 symmetry; B(4) ≡ B(2′), B(5) ≡ B(3′), B(7) ≡ B(9′), and B(8) ≡ B(6′).

Table 14. Selected interatomic angles (°) for [1,1-$(PhMe_2P)_2$-2,4-Cl_2-*closo*-1-NiB_9H_7] with estimated standard deviations in parentheses *

(*a*) At the nickel atom			
P(1)–Ni(1)–P(2)*	103.7(1)		
P(1)–Ni(1)–B(2)	114.1(1)	P(1)–Ni(1)–B(4)*	124.7(1)
P(1)–Ni(1)–B(3)	166.1(1)		
P(1)–Ni(1)–B(5)*	89.0(1)		
B(2)–Ni(1)–B(3)*	52.6(1)	B(2)–Ni(1)–B(5)*	52.1(2)
B(2)–Ni(1)–B(4)*	75.4(1)	B(3)–Ni(1)–B(5)*	79.0(1)
(*b*) Nickel–boron–boron			
Ni(1)–B(2)–B(3)	66.0(2)	Ni(1)–B(5)–B(2)*	61.6(2)
Ni(1)–B(2)–B(5)*	66.3(2)	Ni(1)–B(5)–B(4)*	61.4(2)
Ni(1)–B(2)–B(6)	123.6(2)	Ni(1)–B(5)–B(8)*	119.2(2)
Ni(1)–B(2)–B(9)*	123.6(2)	Ni(1)–B(5)–B(9)*	120.3(2)
(*c*) Other			
Ni(1)–B(2)–Cl(2)	100.2(1)	Ni(1)–B(5)–H(5)*	116.9(18)
Ni(1)–P(1)–C(1)	118.7(1)	B(2)–B(2)–B(5)	94.6(2)
Ni(1)–P(1)–C(7)	111.1(1)	B(2)–B(3)–B(4)	85.4(2)
Ni(1)–P(1)–C(8)	114.8(1)		

* Because of molecular C_2 symmetry, B(4) ≡ B(2′), B(5) ≡ B(3′), B(7) ≡ B(9′), B(8) ≡ B(6′), and P(2) ≡ P(1′).

These two *closo* (rather than *nido* or 'slipped *closo*') metallacarbaborane compounds, however, have structures in which the electron contribution of the metal-atom centre to cluster bonding is generally regarded as two less than in the $[(PhMe_2P)_2NiB_9H_7Cl_2]$ species reported here, *i.e.* $Ni(PR_3)_2$ is a BH-type subrogator. In fact, examination of the disposition of the other ligands about the metal centre in these compounds suggests that there may be significant differences in electronic structure at the metal–borane interface. In the previously reported tetrahapto dicarbaborane species[61] the formal nickel(II) tetragonal bonding plane [as defined by NiP(1)P(2)] bisects the B(2)–B(3) and B(4)–B(5) vectors [structure (**XVIA**)]. The *closo*-structure in these compounds requires the metal centre to contribute two electrons to the NiB_6C_2 cluster bonding which may perhaps thus be interpreted to occur *via* two three-centre two-electron bonds to B(2)B(3) and B(4)B(5) as in structure (**XVIB**), the formal d_{z^2} type lone pair remaining essentially localised on the nickel atom and not

Table 15. Boron-11 n.m.r. data for $[(PhMe_2P)_2NiB_9H_7Cl_2]$[a] in $CDCl_3$ at +21 °C

Assignment[b]	2,4	3,5	6,7,8,9	10
$\delta(^{11}B)$/p.p.m.	+47.4	+26.6[c]	+3.8	+88.6
Relative intensity	2	2	4	1
$^1J(^{11}B-^1H)$/Hz	—	140 ± 10[c]	150 ± 10[c]	130 ± 10

[a] $\delta(^{31}P) = -8.9$ p.p.m. at −51 °C. [b] Based on peak intensities and the absence of coupling $^1J(^{11}B-^1H)$ in the (2,4) resonance. [c] Additional splitting of *ca.* 40 Hz, probably arising from coupling $^2J(^{31}P-Ni-^{11}B)$ (*trans*).

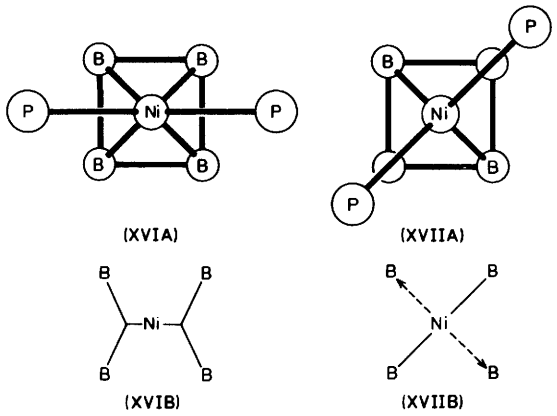

partaking in cluster bonding. In the tetrahapto non-carbon-containing species reported here, by contrast, the metal-atom tetragonal bonding plane [as defined by NiP(1)P(2)] *includes* B(3) and B(5) [structure (**XVIIA**)], and a contribution of four electrons to the cluster could therefore be visualised as arising *via* two formal two-electron two-centre bonds to B(3) and B(5), together with additional bonding interaction of the *dp*-type hybrid electron pair directed towards the electronegatively substituted B(2) and B(4) atoms (**XVIIB**) in a three-centre two-electron bond. This overall interaction may contribute to the very low shielding of the antipodal $^{11}B(10)$ nucleus in this compound (Table 15). A similarly low shielding [$\delta(^{11}B)$ *ca.* +70 p.p.m.] is also observed for the equivalent boron nucleus in the *closo*-species 1-SB_9H_9, in which the antipodal sulphur atom is also regarded as a four-electron cluster contributor.

This is of course a simplistic quasi-valence-bond approach, and structures (**XVIB**) and (**XVIIB**) will represent extreme contributory canonical forms. The difference between these two interpretations is that in the nickel and platinum *closo*-metalladicarbaboranes the metal bonding environment is essentially four-orbital square planar, with a two-orbital contribution to the cluster bonding, whereas in the *closo*-nickelaborane the nickel centre has a five-orbital bonding environment with a *quasi*-conical three-orbital bonding involvement with the cluster. It would be of interest to see a reasonably rigorous molecular-orbital approach to these two contrasting systems, particularly so since it could be argued that the effect of the two chlorine substituents may be such as to stabilise a *closo* species with two fewer electrons than otherwise expected. Non-bonded interaction between the chlorine atoms and the phosphine ligands[36] will also clearly be of significance in determining the observed geometry.

The important general point arising out of these considerations is that metal centres with reasonably flexible valency states and bonding geometries may readily adapt to the different electronic requirements of different clusters: in such cases the rigid application of inflexible 'rules' regarding the supposed electronic and orbital contributions of a particular type of metal centre can be misleading and it is then better to assess each structure individually to determine the forms these contributions might take.[36]

6. *Further Metallaborane Derivatives of* $[(PhMe_2P)_2PtB_8H_{12}]$ *and* $[Pt_2(\mu\text{-}\eta^3\text{-}B_6H_9)_2(PMe_2Ph)_2]$.—Many boranes which contain bridging hydrogen atoms can be readily deprotonated by non-nucleophilic bases such as KH or tmnda and the resulting anions utilised in metathetical reactions with metal–halide species to form metallaborane clusters[16–18,21–23,28,37,38] [equations (5) and (6)].

$$B_nH_m + xKH \longrightarrow [B_nH_{m-x}]^{x-} + xK^+ + xH_2 \quad (5)$$

$$[B_nH_{m-x}]^{x-} + [MX_xL_p] \longrightarrow [L_pMB_nH_{m-x}] + xX^- \quad (6)$$

A number of the metallaboranes reported in this paper themselves contain bridging hydrogen atoms and it was therefore of interest to determine whether these could be similarly deprotonated and further induced to take part in reactions to yield polymetallaborane species. The compounds $[(PhMe_2P)_2PtB_8H_{12}]$ and $[Pt_2(\mu\text{-}\eta^3\text{-}B_6H_9)_2(PMe_2Ph)_2]$ were used as model compounds in these experiments.

$[(PhMe_2P)_2PtB_8H_{12}]$ can be readily deprotonated with KH, and subsequent treatment with *cis*-$[PtCl_2(PMe_2Ph)_2]$ yields the *arachno*-6,9-diplatinadecaborane species $[(PhMe_2P)_4Pt_2B_8H_{10}]$ [equation (7); L = PMe_2Ph, M = Pt]. This

$$[(PhMe_2P)_2PtB_8H_{12}] + 2KH + cis\text{-}[MCl_2L_2] \longrightarrow [(PhMe_2P)_2PtB_8H_{10}ML_2] + 2KCl + H_2 \quad (7)$$

compound, which was the first dimetalladecaborane to be reported, has been adequately described elsewhere[22] and it is of interest to note that it is also formed (but in smaller yield) when $[(PhMe_2P)_2PtB_8H_{12}]$ is treated with base and/or MeOH in the *absence* of *cis*-$[PtCl_2(PMe_2Ph)_2]$. It is a particularly stable species.

In contrast, the analogous reactions with *cis*-$[NiCl_2L_2]$ [equation (7); M = Ni, L = PMe_2Ph or PPh_3], intended to give nickelaplatinadecaborane species, did not occur to any significant extent; instead $[L_4Pt_2B_8H_{10}]$ and/or $[L_2PtB_8H_{12}]$ were formed, *i.e.* products resulting from ligand and/or metal-centre exchange.

The reaction with *cis*-$[PdCl_2(PMe_2Ph)_2]$ [equation (7); M = Pd, L = PMe_2Ph] on the other hand produced intermediate behaviour; the reaction was not clean, but the air-stable 6-palladia-9-platina-*arachno*-decaborane, $[(PhMe_2P)_4PdPtB_8H_{10}]$ was isolated and characterised by n.m.r. spectroscopy. ^1H, ^{11}B, and ^{31}P n.m.r. data are summarised in Tables 16 and 17, and the 40-MHz ^{31}P spectrum is shown in Figure 8. Relative intensities, comparison with data[22] for $[(PhMe_2P)_4Pt_2B_8H_{10}]$, and the incidence of satellite structure arising from $^1J(^{195}Pt-^{11}B)$ = *ca.* 280 Hz (Table 16) led to the stated assignments of the ^{11}B resonances and also confirmed the structure. It is worth noting that the ^{11}B nuclei bound to the first metal in the open face are

Table 16. Boron-11[a] and proton n.m.r. data for the B_8H_{10} moiety in $[(PhMe_2P)_4PdPtB_8H_{10}]$; $CDCl_3$ solution at +21 °C

Assignment[b]	1,3	2	4	5,7	8,10	Bridge
$\delta(^{11}B)$/p.p.m.	−16	+32	+30[c]	+8.5	+2[c]	—
Relative intensity	2	1	1	2	2	—
$\Delta\sigma(^{11}B)$/p.p.m.[d]	−22.2	−7.1	−5.1	−29.2	−22.7	—
$^1J(^{11}B-^1H)$/Hz	135 ± 10	*e*	*e*	*e*	*e*	—
$\delta(^1H)$/p.p.m.	+1.75[f]	+4.95	+5.53	+3.25[f]	+3.05[f]	−1.24
Relative intensity	2	1	1	2	2	2
$^nJ(^{195}Pt-^1H)$/Hz	45 ± 10(^3J)	—	36 ± 5(^2J)	—	*e*	42 ± 5(^2J)

[a] See also Figure 8. [b] Based upon the assigned spectrum of $[(PhMe_2P)_2Pt_2B_8H_{10}]$ (ref. 22). [c] Coupling to ^{195}Pt *ca.* 280 Hz (estimated). [d] $\Delta\sigma$ = substituent shielding effect = $\delta(B_8H_{14}) - \delta[(PhMe_2P)_4PdPtB_8H_{10}]$ (see Table 1, footnote *c*). [e] Not measurable due to overlapping and/or broad resonances. [f] Tentative.

Table 17. Phosphorus-31 and proton n.m.r. data for $[(PhMe_2P)_4PdPtB_8H_{10}]$

Assignment	$Pd(PMe_2Ph)_2$		$Pt(PMe_2Ph)_2$	
$\delta(^{31}P)$/p.p.m.[a]	−14.8		−5.9	
$^1J(^{195}Pt-^{31}P)$/Hz	—		+2 755 ± 5	
$^4J(^{195}Pt-^{31}P)$/Hz	5 ± 2		—	
$^5N(^{31}P-^{31}P)$/Hz[b]	30 ± 2		30 ± 2	
$\delta(^1H)$(MeP)/p.p.m.[c,d]	+1.45 (A)	+1.33 (B)	+1.70 (C)	+1.55 (D)
$^3J(^{195}Pt-^1H)$/Hz	—	—	26 ± 1 (C)	24.4 ± 0.5 (D)
$[^2J(^{31}P-^1H) + {}^4J(^{31}P-^1H)]$/Hz	7.4 ± 0.5 (A)	7.1 ± 0.5 (B)	7.6 ± 0.5 (C)	8.3 ± 0.5 (D)

[a] In $CDCl_3$ solution at −40 °C. [b] ^5J (*cis*) and ^5J (*trans*) probably of same sign and similar magnitude [see also refs. 22 and 36(*b*)]. [c] Four inequivalent P-methyl groups (A—D) arising from the prochirality at the metal sites. [d] In $CDCl_3$ solution at +21 °C.

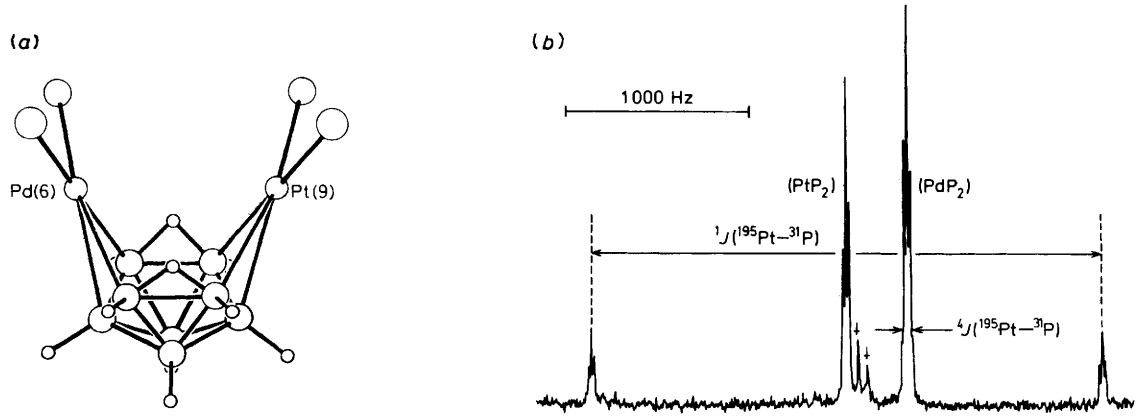

Figure 8. (*a*) A representation of the structure of the cluster of $[(PhMe_2P)_4PdPtB_8H_{10}]$ and (*b*) its 40.25-MHz $^{31}P-\{^1H(broad\ band\ noise)\}$ n.m.r. spectrum at −43 °C in $CDCl_3$ solution (impurity peaks are denoted by ↓). The spectrum shows the effects of both long- and short-range couplings between ^{195}Pt and ^{31}P. The effects of coupling $^5J(^{31}P-^{31}P)$ are also apparent; the triplet structure is 'deceptively simple' since $^5J(^{31}P-^{31}P)(cis)$ and $^5J(^{31}P-^{31}P)(trans)$ arise from different coupling paths and the four ^{31}P nuclei constitute an $[AX]_2$ spin system

only deshielded by *ca.* 3 p.p.m. on addition of a second metal centre, as compared with either of the monometal species. Also the resonance assigned to the boron atoms B(9,8) (*i.e.*, those bonded to the platinum in the open face) at $\delta(^{11}B)$ +2 p.p.m. is not dissimilar to that for the corresponding B(5,9) atoms in the monoplatinum species $[(PhMe_2P)_2PtB_8H_{12}]$ at $\delta(^{11}B)$ −1.7 p.p.m. The same is true of the boron atoms bonded to the palladium at $\delta(^{11}B)$ +8.5 p.p.m. (dimetal species) and +5.5 p.p.m. (monopalladium species), again consistent with the assignment. The phosphine methyl proton n.m.r. behaviour was also consistent with the formulation as was the ^{31}P n.m.r. behaviour, which in particular exhibited long-range couplings $^5J[^{31}P(Pd)-^{31}P(Pt)]$ together with both long-range and short-range couplings $^4J(^{195}Pt-^{31}P)$ and $^1J(^{195}Pt-^{31}P)$. It is of interest to note that, following the initial report of compounds of this type,[22] dimetalladecaboranes of both the *nido* and *arachno* variety are now commonplace[16,36,38] but this is the first dimetalladecaborane of any kind containing two different metals, and the only metallaborane of any kind to contain metals from two different periods of the Periodic Table.*

Attempts to use other metal centres in reaction (7) have so far not been successful, although it may be noted that the corresponding platinairidadecaborane $[(Me_3P)_2PtB_8H_{10}Ir(PMe_3)_2(CO)H]$ can be prepared by an analogous reaction of a corresponding iradanonaborane species [equation (8)]; this is described more thoroughly elsewhere.[36]

$$[H(OC)(Me_3P)_2IrB_8H_{12}] + 2KH + [PtCl_2(PMe_3)_2] \longrightarrow 2KCl + H_2 + [(Me_3P)_2PtB_8H_{10}Ir(PMe_3)_2(CO)H] \quad (8)$$

* *Note added in proof.* Since the submission of this paper, a ruthenium–osmium–decaborane species has been reported by M. Elrington, N. N. Greenwood, J. D. Kennedy, and M. Thornton-Pett, *J. Chem. Soc., Chem Commun.*, 1984, 1398.

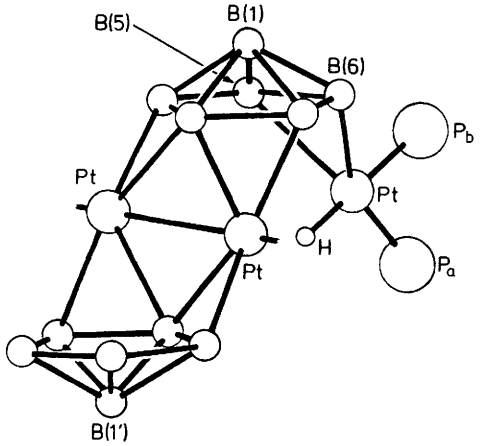

Figure 9. Schematic representation of the $Pt_2(B_6H_9)\{B_6H_8[Pt(PMe_2Ph)_2H]\}$ unit of $[Pt_2(\mu\text{-}\eta^3\text{-}B_6H_9)(\mu\text{-}\{\eta^3\text{-}B_6H_8\text{-}\eta^2\text{-}[PtH\text{-}cis\text{-}(PMe_2Ph)_2]\})(PMe_2Ph)_2]$, with borane-H atoms and P-organo-groups omitted for clarity

Initial experiments have also indicated that further polymetallaborane species can be synthesised from the dimeric *conjuncto* species $[Pt_2(\mu\text{-}\eta^3\text{-}B_6H_9)_2(PMe_2Ph)_2]$, in which the two B_6H_9 clusters each have three sites bridged by hydrogen atoms which are in principle available for deprotonation and subsequent co-ordination to suitable positive metal centres. For example, treatment of $[Pt_2(\mu\text{-}\eta^3\text{-}B_6H_9)_2(PMe_2Ph)_2]$ with base (KH or tmnda) followed by reaction with *cis*-$[PtCl_2(PMe_2Ph)_2]$ results in the production, in small yields (*ca.* 10%), of a yellow solid compound which n.m.r. spectroscopy (as discussed in the following paragraph) indicates is $[Pt_2(\mu\text{-}\eta^3\text{-}B_6H_9)(\mu\text{-}\{\eta^3\text{-}B_6H_8\text{-}\eta^2\text{-}[PtH\text{-}cis\text{-}(PMe_2Ph)_2]\})(PMe_2Ph)_2]$, *i.e.* a bridging hydrogen atom in $[Pt_2(\mu\text{-}\eta^3\text{-}B_6H_9)_2(PMe_2Ph)_2]$ has been replaced by a bond to the *cis*-$PtH(PMe_2Ph)_2$ moiety (Figure 9).

Phosphorus-31 n.m.r. data for this compound are summarised in Table 18 and the 40-MHz $^{31}P\text{-}\{^1H(\text{broad band})\}$ n.m.r. spectrum is given in Figure 10. The symmetrical linear P–Pt–Pt–P system is clearly retained in the product, and the overall similarity of the parameters associated with this trimetallaborane system to those of the parent dimetallaborane

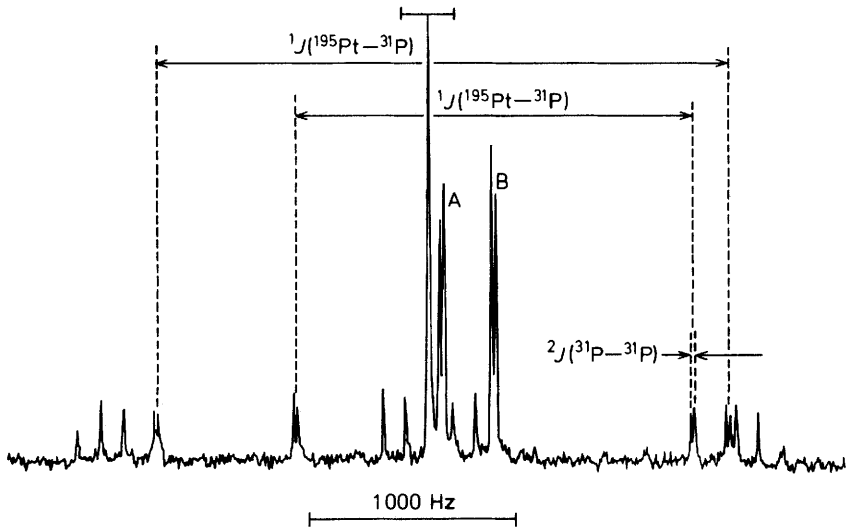

Figure 10. 40.25-MHz $^{31}P\text{-}\{^1H(\text{broad band noise})\}$ n.m.r. spectrum of $[Pt_2(\mu\text{-}\eta^3\text{-}B_6H_9)(\mu\text{-}\{\eta^3\text{-}B_6H_8\text{-}\eta^2\text{-}[PtH\text{-}cis\text{-}(PMe_2Ph)_2]\})(PMe_2Ph)_2]$ in CD_2Cl_2 solution at −60 °C. The sub-spectrum arising from the linear P–Pt–Pt–P system is not labelled in this diagram and is basically similar to that of unsubstituted $[Pt_2(B_6H_9)_2(PMe_2Ph)_2]$ (Figure 6); this indicates substitution on the molecular mirror plane. The labelled ^{195}Pt satellite positions (– – –) arise from the η^2-PtH-*cis*-$(PMe_2Ph)_2$ moiety; for this there are two different ^{31}P central resonance positions, **AB**, with mutual coupling $^2J(^{31}P-^{31}P)(cis)$ of 17 Hz. The different couplings $^1J(^{195}Pt-^{31}P)$ reflect the different *trans*-influences of the Pt–H and the Pt–η^2-B_2 bonding modes

Table 18. Phosphorus-31[a] and proton[b] n.m.r. data for $[Pt_2(\mu\text{-}\eta^3\text{-}B_6H_9)(\mu\text{-}\{\eta^3\text{-}B_6H_8\text{-}\eta^2\text{-}[PtH\text{-}cis\text{-}(PMe_2Ph)_2]\})(PMe_2Ph)_2]$

	P_a *trans* to borane	P_b *trans* to hydride	P–Pt–Pt–P
$\delta(^{31}P)$/p.p.m.	−2.1	−8.0	−0.7
$^1J(^{195}Pt-^{31}P)$/Hz	+2 601 ± 5	+1 804 ± 5	+2 888 ± 5
$^2J(^{31}P-^{31}P)$/Hz	17 ± 2	17 ± 2	—
$^2J(^{195}Pt-^{31}P)$/Hz	—	—	+317.5 ± 2
$^3J(^{31}P-^{31}P)$/Hz	—	—	159 ± 2
$^4J(^{195}Pt-^{31}P)$/Hz	5 ± 2	5 ± 2	*c*
$\delta(^1H)$(MeP)/p.p.m.	+1.54	+1.64	+2.13
$^3J(^{195}Pt-^1H)$/Hz	36 ± 1	*ca.* 20?[d]	28 ± 1
Hydride			
$\delta(^1H)$/p.p.m.	−6.3		
$^1J(^{195}Pt-^1H)$/Hz	834 ± 5		
$^2J(^{31}P-^1H)(trans)$/Hz	206 ± 5		
$^2J(^{31}P-^1H)(cis)$/Hz	17 ± 1		

[a] In $CDCl_3$ solution at −40 °C (see also Figure 10). [b] In $CDCl_3$ solution at +21 °C. [c] No apparent satellites observed. [d] Estimated (lines not well resolved under the conditions used).

Table 19. Proton and boron-11 n.m.r. data for $[Pt_2(\mu\text{-}\eta^3\text{-}B_6H_9)(\mu\text{-}\{\eta^3\text{-}B_6H_8\text{-}\eta^2\text{-}[PtH\text{-}cis\text{-}(PMe_2Ph)_2]\})(PMe_2Ph)_2]$ in $CDCl_3$ solution at +21 °C

	^1H		^{11}B	
Assignment[a]	δ/p.p.m.[b]	Relative intensity	δ/p.p.m.[c]	Relative intensity
1	+1.2	1	−32	1
1′	+0.65	1	−44	1
3	+6.3	1	+56	1
3′	+6.7	1	+61	1
2,4	+3.3	2	−5	2
2′,4′	+2.85	2	+1	2
5,6	+4.2	2	+4	2
5′,6′	+4.25	2	+7	2
Bridging				
(2,6),(2′,6′)	−0.15	2	—	—
(4,5),(4′,5′)	−0.75	2	—	—
(5,6)	−1.15	1	—	—

[a] See text; numbering based upon $[Pt_2(\mu\text{-}\eta^3\text{-}B_6H_9)_2(PMe_2Ph)_2]$ (Table 5 and Figures 4 and 9); unprimed numbers refer to the sub-cluster bearing the third platinum substituent. [b] δ(^1H) quoted ±0.1 p.p.m. [c] δ(^{11}B) quoted ±1 p.p.m.

(Table 6) shows that platinum substitution on the borane cage does not have particularly severe effects on the general cluster bonding; in addition the retention of the ^{31}P spectroscopic symmetry indicates that the new site of substitution does not introduce molecular asymmetry and is therefore presumably at the (5,6)-bridging position on one of the hexaborane clusters. This conclusion is supported by the proton n.m.r. data discussed below.

In addition to the above lines, the ^{31}P n.m.r. spectrum also contains lines arising from the phosphine ligands bound to the third, substituent, platinum atom. These resemble the general pattern previously found for *cis*-bis(phosphine)platinum(II) complexes of pentaborane(9),[17,18] $[Pt(PMe_2Ph)_2X(B_5H_8)]$, which also have the platinum atom in a basal bridging position on the *nido*-borane cluster. This pattern consists of two central resonances, one broader (*trans* to borane) and one sharper (*trans* to X), exhibiting mutual coupling $^2J(^{31}P\text{–}^{31}P)(cis)$, these lines being flanked by satellites arising from couplings $^1J(^{195}Pt\text{–}^{31}P)$. In the present compound, the coupling $^1J(^{195}Pt\text{–}^{31}P)$ (*trans* to X) is particularly low, *ca.* 1 800 Hz, suggesting that X is a substituent with a very large *trans* effect, *viz.* hydride, and this was confirmed by ^1H n.m.r. spectroscopy as summarised below. The *trans* effects as apparent from this compound fit nicely into the sequences previously established,[13,17,18,27,62,63] *viz.*, σ-B > H ~ alkyl > μ-BB ≫ halogen.

It may also be noted that the ^{31}P spectra exhibit effects which may arise from long-range couplings, $^4J(^{195}Pt\text{–}B\text{–}B\text{–}Pt\text{–}^{31}P)$, of *ca.* 5 Hz {somewhat analogous to those mentioned above for $[(PhMe_2P)_4PtPdB_8H_{10}]$}, but we have not been able to resolve these unequivocally.

The boron-11 n.m.r. data (Table 19) are also consistent with the structure of Figure 9. The individual B(2,4), B(5,6), B(2′4′), and B(5′,6′) resonances were not resolved at 32 MHz, but the two apical B(1) and B(1′) resonances are readily distinguishable; one occurring at δ(^{11}B) = *ca.* −43.4 p.p.m., very similar to that of the parent compound and ascribable to the unsubstituted B_6H_9 cluster, the second at −31.9 p.p.m., corresponding to the platinum-substituted B_6H_8 cluster, the downfield shift being similar to that generally associated with apical boron atoms on formation of μ-bridged transition-metal species from B_6H_{10} and B_5H_9.[17,39,40] The 100-MHz proton n.m.r. spectrum is also consistent with the proposed formulation (Table 19); again the resonances ascribed to the (2,4), (5,6), (2′,4′), and 5′,6′) protons were not individually resolved but the 4:2 intensity pattern of the bridging protons in the diplatinum parent compound (Table 5) had given way to the 2:2:1 ratio expected for the symmetrical product. In addition the Pt–hydride resonance at δ −6.3 p.p.m. ($CDCl_3$ solution) is readily apparent (Table 18). The presence of the platinum hydride is of interest, but it does not necessarily arise from the KH used in the initial deprotonation, as the same Pt–hydride product is also produced when the non-hydridic tmnda is used as base. This together with the low yield suggests that the reaction may involve more than a straightforward metathesis.

The formally tridentate (*i.e.* bidentate/monodentate) trihapto–dihapto bonding mode of the B_6H_8 cluster is unique and novel in hexaborane chemistry, although as mentioned above monodentate dihapto has been well characterised[16–18,39,40] and bis(monodentate) bis(dihapto) also probably occurs.[16,41] The structure of the nine-vertex $Pt_3B_6H_8$ sub-cluster, (**XVIII**), has an arrangement of vertices similar to that of the *arachno-n*-B_9H_{15} molecule, (**XIX**). It is not clear whether the overall

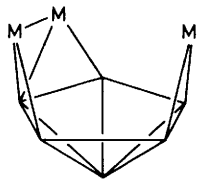

(XVIII)

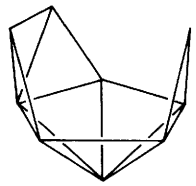

(XIX)

$[L_4Pt_3B_{12}H_{18}]$ compound should be regarded as a 15-vertex *hypho* ($n + 4$) or a *klado* ($n + 5$) trimetallapentadecaborane species but, as discussed above, these descriptions have limited use and meaning in extended *conjuncto* macropolyhedral systems such as these.

The reaction of $[Pt_2(\mu\text{-}\eta^3\text{-}B_6H_9)_2(PMe_2Ph)_2]$ with a number of other transition-metal complexes has so far not yielded any further trimetallaboranes, but an interesting side reaction when PPh_3 metal complexes are used is the formation of a mixed phosphine–diplatinum species $[Pt_2(\mu\text{-}\eta^3\text{-}B_6H_9)_2(PMe_2Ph)(PPh_3)]$, which was characterised by ^{31}P and ^{11}B n.m.r. spectroscopy (see Tables 20 and 21 respectively).

7. *Additional Considerations and some General Conclusions.*— Several points arising out of the above work merit some additional comment.

Of obvious interest is the mechanistic route by which the nine-, eight-, and six-boron clusters are formed from reactions involving the ten-vertex oxyborane species. It seems likely that the reactions may proceed *via arachno* nine-vertex species such as $[B_9H_{14}]^-$, since this is known to be the major degradation product of $(B_{10}H_{13})_2O$ even under very mildly basic conditions,[3] and also the nature and distribution of the products in the reactions reported above are to a large extent very similar to those in the reactions of *cis*-$[PtCl_2(PMe_2Ph)_2]$ with the $[B_9H_{14}]^-$ anion[22] and other *arachno* and *nido* nine-vertex borane species.[25,29,32,34,36,38]

We have indications from other work being carried out in these laboratories[16,25,38] that the *arachno*-$[(PhMe_2P)_2PtB_8H_{12}]$ product may be formed *via* an initial attack of the Pt moiety at the (6,5,9) region of the *iso-arachno* nine-vertex cluster [equation (9)], accompanied by expulsion of the opposing B(7) vertex; if this is so then the fate of the B(7) atom is of interest, although no clear-cut explanation is available at this time.

Table 20. Phosphorus-31 n.m.r. data for $[Pt_2(\mu\text{-}\eta^3\text{-}B_6H_9)_2(PMe_2Ph)(PPh_3)]$ in $CDCl_3$ solution at −40 °C

Assignment	PPh_3*	PMe_2Ph*
$\delta(^{31}P)$/p.p.m.	+39.7 ± 0.5	+0.9 ± 0.5
$^1J(^{195}Pt\text{–}^{31}P)$/Hz	+2 844 ± 5	+2 840 ± 5
$^2J(^{195}Pt\text{–}^{31}P)$/Hz	+380 ± 5	+320 ± 5
$^3J(^{31}P\text{–}^{31}P)$/Hz	101 ± 2	101 ± 2

* Based upon comparison of ^{31}P n.m.r. data from $[Pt_2(\mu\text{-}\eta^3\text{-}B_6H_9)_2(PMe_2Ph)_2]$ (Table 6) and $[Pt_2(\mu\text{-}\eta^3\text{-}B_6H_9)_2(PPh_3)_2]$ (Table 7).

Table 21. Boron-11 n.m.r. data for $[Pt_2(\mu\text{-}\eta^3\text{-}B_6H_9)_2(PMe_2Ph)(PPh_3)]$ in $CDCl_3$ solution at +21 °C

Assignment[a]	1	2,4	3	5,6
$\delta(^{11}B)$/p.p.m.[b]	−41.9	−2.9	+60.5	+6.7
Relative intensity	1	2	1	2
$^1J(^{11}B\text{–}^1H)$/Hz	c	c	c	130 ± 20

[a] Based upon the assigned spectrum of $[Pt_2(\mu\text{-}\eta^3\text{-}B_6H_9)_2(PMe_2Ph)_2]$ (Table 5). [b] Broad resonances, $\delta(^{11}B)$ ±1.5 p.p.m. [c] Not measured due to broad resonances.

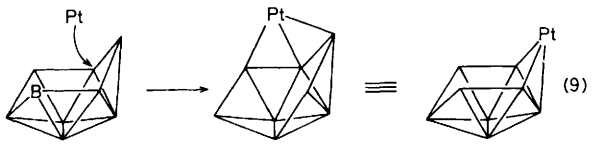

However, it may be significant that the reaction to give $[(PhMe_2P)_2PtB_8H_{12}]$ from $[B_9H_{14}]^-$ in aprotic solvents produces the highest yield when the ratio of $[B_9H_{14}]^-$ to *cis*-$[PtCl_2(PMe_2Ph)_2]$ is 2:1.[22] This is of interest, since this stoicheiometry implies the production of the as yet uncharacterised *arachno* decaborane, $B_{10}H_{16}$, under mild conditions [equation (10)]. We hope to report more conclusively on this interesting possibility in a future communication. Also when a 1:1 ratio of reactants is used in methanolic solution the reaction proceeds smoothly and is the most convenient route to this compound; presumably in this case the B(7) vertex is abstracted by the MeOH with a probable stoicheiometry as indicated in equation (11).

$$cis\text{-}[PtCl_2(PMe_2Ph)_2] + 2[B_9H_{14}]^- \longrightarrow [(PhMe_2P)_2PtB_8H_{12}] + \{B_{10}H_{16}\} + 2Cl^- \quad (10)$$

$$cis\text{-}[PtCl_2(PMe_2Ph)_2] + [B_9H_{14}]^- \xrightarrow{MeOH} [(PhMe_2P)_2PtB_8H_{12}] + HCl + B(OMe)_3 + 2{\cdot}5H_2 \quad (11)$$

The formation of the diplatinaborane cluster species $[Pt_2(\mu\text{-}\eta^3\text{-}B_6H_9)_2(PMe_2Ph)_2]$ is also of interest. It seems to be a particularly stable species, and since its initial characterisation [7] we have detected its presence in many reaction systems involving higher boranes and phosphine–platinum species.[16,22–25,38] It is not clear at present whether in this reaction it is formed independently of the platinanonaborane species or as a degradation or other product thereof; recent work in these laboratories[24,38] has shown that it is a product, in minor yield, of the thermolysis of $[(PhMe_2P)_2PtB_8H_{12}]$ at 110 °C, but these conditions are far removed from those of the reactions discussed here. It seems most likely to result from further attack

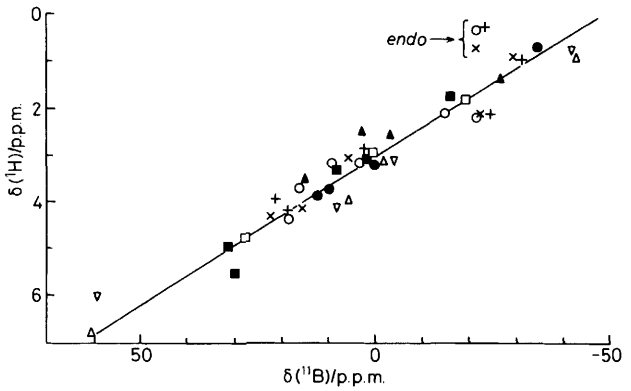

Figure 11. Proton–boron-11 nuclear shielding correlation plot (with bridging protons omitted) for the compounds $[(PhMe_2P)_2PdB_8H_{12}]$ (X), $B_{10}H_{14}$ (●), $PhMe_2P{\cdot}B_9H_{13}$ (○), $[(PhMe_2P)_4PtPdB_8H_{10}]$ (■), $[(PhMe_2P)_4Pt_2B_8H_{10}]$ (□), $[(PhMe_2P)_2PtB_{10}H_{12}]$ (▲), $[(PhMe_2P)_2PtB_8H_{12}]$ (+), $[(PhMe_2P)_2Pt_2(B_6H_9)_2]$ (△), and $[(Ph_3P)_2Pt_2(B_6H_9)_2]$ (▽). The line drawn represents the ratio $\delta(^{11}B):\delta(^1H) = 16:1$

at a platinum centre on a preformed platinaborane, and (admittedly very general) schemes such as (12) which would

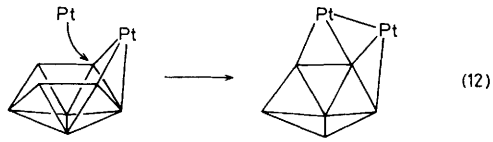

involve platinum attack at the (7,8,9) positions are attractive possibilities for the initial formation of the Pt–Pt bond.

A further general aspect that merits discussion concerns the ^1H and ^{11}B n.m.r. data that we have been able to obtain for the variety of polyhedral species discussed above. By use of $^1H\text{-}\{^{11}B\}$ spectroscopy [4,13,19,22] we have been able easily to assign the terminal hydrogen atoms to the boron nuclei to which they are directly bonded. Previous to our work, this type of information was limited to only a few compounds which had been examined by use of this technique, or for which the assignments had been established by other methods, such as labelling, comparison of resolved coupling constants, multiplicities, symmetries, *etc.*

In Figure 11 are plotted $\delta(^{11}B)$ *versus* $\delta(^1H)$ for selected compounds reported above plus a number of other related species. It is apparent that the general correlation between $\delta(^{11}B)$ and $\delta(^1H)$, noted some years ago,[64] and more specifically more recently for one or two isolated individual species,[4,19,22,26] seems to hold. In particular the resonances for $(^{11}B,^1H)(3)$ in $[Pt_2(\mu\text{-}\eta^3\text{-}B_6H_9)_2L_2]$ (L = PMe_2Ph or PPh_3) do not deviate significantly from the general trend, even though the ^{11}B nucleus resonates at very low field and is between two platinum atoms, and therefore may be expected to have an anomalous electronic environment and consequent anomalous shielding behaviour. It is noted that the *endo*-terminal protons generally lie *ca.* 2 p.p.m. above the general trend, which is a useful diagnostic for *arachno* systems, and that bridging protons (not plotted) are still higher, but that the *exo*-terminal protons generally do not deviate from the trend except by amounts that are compatible with reasonable local anisotropic variations in the ^1H shielding environment.[26] However, it should be borne in mind that the compounds in this plot may well not be entirely representative; for example there are no *closo* or *hypho* species, and within the *arachno* and *nido* clusters represented there is only a limited representation of known types.

Experimental

General.—Reactions were carried out in an atmosphere of dry nitrogen, although (except where indicated) subsequent work-up was carried out under less rigorous conditions. Solvents were distilled from drying agents under nitrogen before use. *nido*-Decaborane was obtained commercially and purified by sublimation before use. Complexes of the type *cis*-$[MCl_2L_2]$ (M = Ni, Pd, or Pt; L = PMe_2Ph or PPh_3) were prepared by standard literature methods.[65] KH was obtained commercially and freed from mineral oil by washing with pentane before use. SMe_2 was used as supplied and $B_{10}H_{12}(SMe_2)_2$ was prepared by standard methods.[26] Thin-layer chromatography (t.l.c.) was carried out on plates prepared in the laboratory as required, from silica gel [Kieselgel 60G (Merck)]. General chromatographic techniques were as described in previous reports from these laboratories.[22,66] Infrared spectra were recorded using KBr discs on a Perkin-Elmer 457 grating instrument and $\nu_{max.}$ are quoted ± 5 cm^{-1}. Melting points were determined in open capillary tubes. Yields are quoted with respect to the metal complexes except where this is obviously inappropriate, in which case they are with respect to the borane species.

Nuclear Magnetic Resonance Spectroscopy.—100-MHz ^1H, ^1H-$\{^{11}B\}$, and ^1H-$\{^{31}P\}$; 32-MHz ^{11}B and ^{11}B-$\{H\}$; and 40-MHz ^{31}P-$\{^1H\}$ experiments were carried out on a JEOL FX-100 pulse (Fourier-transform) spectrometer equipped for double resonance. The 128-MHz ^{11}B and ^{11}B-$\{^1H\}$ n.m.r. spectra were recorded on the Bruker WH400 SERC service instrument at the Department of Chemistry, University of Sheffield. The spectra were typically recorded for $CDCl_3$ solutions at 21 °C unless otherwise stated. Chemical shifts (δ) are given in p.p.m., to low frequency ('high field') of $SiMe_4$ for ^1H, of $Et_2O{\cdot}BF_3$ in $CDCl_3$ for ^{11}B (Ξ 32 083 971 Hz),[13] and of 85% H_3PO_4 (Ξ 40 480 730 Hz) for ^{31}P. Boron chemical shifts are given ± 1 p.p.m., phosphorus chemical shifts ± 0.5 p.p.m., and proton chemical shifts ± 0.05 p.p.m. unless otherwise stated. Boron-11 longitudinal relaxation times, $T_1(^{11}B)$, were measured at 32 MHz using the π-τ-$\pi/2$ pulse sequence together with the null method.[66,67] The π and $\pi/2$ pulses measured for the samples used were found to be 32 and 16 μs respectively. The $\{X\}$ irradiation power levels used in selective ^1H-$\{X\}$ experiments had previously[4,19] been optimised by trial and error on known compounds for each particular type of decoupling experiment: $\gamma B_2/2\pi$ as estimated by off-resonance residual splitting[67] was of the order of a few hundred Hz in the selective ^1H-$\{^{11}B\}$ decoupling experiments but the irradiation conditions were not particularly critical in the work reported here.

Mass Spectroscopy.—The mass spectra were recorded on an AEI/Kratos MS30 mass spectrometer using a solid-sample probe insert at a nominal ionising voltage of 70 eV.

***Preparation and Isolation of* 6,6′-$(B_{10}H_{13})_2O$ *and* 6-$B_{10}H_{13}OH$.**—The method reported here is essentially the same as that reported for the synthesis of 6,6′-$(B_{10}H_{13})_2O$, by Heřmánek *et al.*,[3] except for a crucial modification in work-up procedure.

$B_{10}H_{12}(SMe_2)_2$ (2.4 g, 9.8 mmol) was dissolved in benzene (*ca.* 10 cm^3) in a separating funnel, and to this was added 98% H_2SO_4 (2 cm^3). The mixture was agitated vigorously for 10 min at room temperature; the acid layer was then removed and a fresh portion of 98% H_2SO_4 added. This procedure was repeated with a total of five portions. The combined acid portions were then extracted with benzene (2×5 cm^3). The combined extracts were dried ($MgSO_4$). After filtration, the benzene was removed under reduced pressure (*ca.* 25 °C/5 mmHg) and the white deposit was extracted twice with hot cyclohexane (*ca.* 50 cm^3). After cooling, the white precipitate was collected and a second crop was subsequently collected by reducing the volume of cyclohexane. The combined crops were washed with pentane and dried *in vacuo*. The material had a poorly defined melting point (130—135 °C) and was sublimed (100—120°/10 °C, 10^{-3} mmHg) for up to 2 weeks. The sublimed material was pure 6,6′-$(B_{10}H_{13})_2O$ (0.66 g, 2.5 mmol, 26%), m.p. 139—140 °C; ν(B–H) 2 580s, 2 570s, and 2 540s cm^{-1}. The unsublimed residue was recrystallised twice from hot cyclohexane to yield the white, hygroscopic compound, 6-$B_{10}H_{13}OH$ (0.35 g, 2.5 mmol, 26%), m.p. (decomp.) > 160 °C; ν(B–H) 2 570s, 2 530s; ν(O–H) 3 570m cm^{-1}.

Interconversion Reactions.—(a) 6-$B_{10}H_{13}OH$ (0.05 g, 0.36 mmol) was refluxed in benzene solution (*ca.* 20 cm^3) for 16 h using a Dean and Stark apparatus. The benzene was then removed under reduced pressure and only unreacted 6-$B_{10}H_{13}OH$ could be extracted from the residue.

(b) Four portions of 6-$B_{10}H_{13}OH$ (0.05 g, 0.36 mmol) were each dissolved in benzene (*ca.* 20 cm^3) and to each was added one of the following: P_2O_5 (1 g), 5% oleum (1 cm^3), 98% H_2SO_4 (1 cm^3), or 50% H_2SO_4 (1 cm^3). After stirring for 4 h, the benzene layers were separated, dried ($MgSO_4$), and the benzene then removed under reduced pressure. The residual white solids yielded only 6-$B_{10}H_{13}OH$ upon extraction.

(c) 6,6′-$(B_{10}H_{13})_2O$ (0.05 g, 20 mmol) was dissolved in benzene (*ca.* 20 cm^3) and stirred for 4 h with 98% H_2SO_4 (1 cm^3). The organic layer was separated, dried ($MgSO_4$), and the benzene then removed under reduced pressure, yielding only 6,6′-$(B_{10}H_{13})_2O$. A similar procedure with 50% H_2SO_4 (1 cm^3) yielded 6,6′-$(B_{10}H_{13})_2O$ with a minute trace of 6-$B_{10}H_{13}OH$.

Reactions of 6-$B_{10}H_{13}OH$ *and* 6,6′-$(B_{10}H_{13})_2O$.—(a) *With bromine.* 6-$B_{10}H_{13}OH$ (0.05 g, 0.36 mmol) was dissolved in benzene (*ca.* 20 cm^3) and bromine (2 cm^3) was distilled on at −196 °C. The solution was stirred at *ca.* 20 °C for 16 h, after which the more volatile components were removed under reduced pressure. The residue was insoluble in organic solvents. 6,6′-$(B_{10}H_{13})_2O$ (0.1 g, 0.39 mmol) was treated under similar conditions and the residue was extracted with hot cyclohexane to yield only unreacted 6,6′-$(B_{10}H_{13})_2O$ (0.094 g, 0.36 mmol, 94% recovery), m.p. 136—137 °C.

(b) *With Phosphorus pentachloride.* 6-$B_{10}H_{13}OH$ (0.05 g, 0.36 mmol) was dissolved in benzene (*ca.* 20 cm^3) and to this was added an excess of PCl_5 (1 g). After heating the mixture under reflux for 16 h the solvent was removed under reduced pressure. Extraction of the residue with hot cyclohexane (*ca.* 20 cm^3) yielded a *ca.* 1:1 mixture of 6-$B_{10}H_{13}OH$ and 6-$B_{10}H_{13}Cl$, identified and analysed by integrated n.m.r. spectroscopy. A similar treatment of 6,6′-$(B_{10}H_{13})_2O$ (0.1 g, 0.39 mmol) yielded only unreacted 6,6′-$(B_{10}H_{13})_2O$ (0.074 g, 0.29 mmol, 74%), m.p. 136—138 °C, after cyclohexane extraction.

(c) *With* N,N,N′,N′-*tetramethylnaphthalene*-1,8-*diamine* (*tmnda*) ('*proton sponge*'). 6-$B_{10}H_{13}OH$ (0.05 g, 0.36 mmol) was dissolved in CH_2Cl_2 (*ca.* 20 cm^3) and to this was added 'proton sponge' (0.08 g, 0.37 mmol). After 1 h a white precipitate was filtered off and identified as $B(OH)_3$. To the liquor was added pentane (10 cm^3) and the resulting white precipitate was collected by filtration and identified as [Htmnda][B_9H_{14}] (0.094 g, 0.3 mmol, 80%). 6,6′-$(B_{10}H_{13})_2O$ (0.1 g, 0.39 mmol) was dissolved in CH_2Cl_2 (*ca.* 20 cm^3) and to this was added 'proton sponge' (0.167 g, 0.78 mmol). After *ca.* 30 min stirring a yellow colouration developed, which after 2 h was replaced by a white precipitate which was collected and identified as $B(OH)_3$. Addition of pentane (10 cm^3) to the liquor resulted in the precipitation of [Htmnda][B_9H_{14}] (0.12 g, 0.4 mmol, 48%). Treatment of 6,6′-$(B_{10}H_{13})_2O$ (0.1 g, 0.39 mmol) with 'proton

sponge' (0.167 g, 0.78 mmol) in methanol (*ca.* 20 cm^3) yielded a yellow solution. Removal of the more volatile components under reduced pressure gave $[Htmnda][B_9H_{14}]$ (0.1 g, 0.3 mmol, 38%) and $[Htmnda][B_3H_8]$ (0.09 g, 0.35 mmol, 40%). The volatile fractions contained $B(OMe)_3$.

Reactions of $6,6'$-$(B_{10}H_{13})_2O$, 6-$B_{10}H_{13}OH$, *or* $[NMe_4][B_9H_{14}]$ *with cis*-$[MCl_2L_2]$ (M = Ni, Pd, *or* Pt; L = PMe_2Ph *or* PPh_3).—General techniques for these reactions were as described in a previous publication.[22]

1. *Reactions of* $6,6'$-$(B_{10}H_{13})_2O$. (a) *With cis*-$[PtCl_2(PMe_2Ph)_2]$. A solution of *cis*-$[PtCl_2(PMe_2Ph)_2]$ (0.21 g, 0.38 mmol) and $6,6'$-$(B_{10}H_{13})_2O$ (0.10 g, 0.38 mmol) in CH_2Cl_2–Et_2O (1:1, *ca.* 20 cm^3) was stirred at 20 °C for 72 h, then filtered through silica gel [Kieselgel 60 (Merck), 0.063—0.200 mm mesh; *ca.* 5 g], and washed through with light petroleum (b.p. 60—80 °C)—CH_2Cl_2 (1:1, *ca.* 100 cm^3). The more volatile components were then removed from the combined filtrates under reduced pressure and the product mixture separated using repeated preparative scale t.l.c. with light petroleum (b.p. 60—80 °C)—CH_2Cl_2 (1:1) as eluant. This yielded a number of products, including bis(dimethylphosphine)-di-μ-(2,3,4-η^3-*nido*-hexaboranyl)-diplatinum, $[Pt_2(\mu\text{-}\eta^3\text{-}B_6H_9)_2(PMe_2Ph)_2]$ (10 mg, 0.013 mmol, 3.6%, R_f 0.42) [Found: C, 23.3; H, 5.0; B, 16.3; P, 7.8; Pt (by difference), 47.6. $C_{16}H_{40}B_{12}P_2Pt_2$ requires C, 23.3; H, 4.9; B, 16.0; P, 7.6; Pt, 47.9%]. Infrared: ν(B–H), 2 580m, 2 570m, 2 550m, 2 518m, and 2 500m cm^{-1}. Raman: ν(Pt–Pt), 185 cm^{-1}. M.p. (decomp.) >200 °C. Recrystallisation from a CH_2Cl_2–cyclohexane mixture yielded yellow needles, one of which was suitable for *X*-ray diffraction experiments. Also isolated were larger quantities of 4,4-bis(dimethylphenylphosphine)-*arachno*-4-platinanonaborane, $[(PhMe_2P)_2PtB_8H_{12}]$ (*ca.* 25 mg, 0.044 mmol, 10.5%, R_f 0.35). Recrystallisation from hot benzene yielded crystals suitable for *X*-ray diffraction experiments described elsewhere (ref. 22) (see Figure 3). A smaller quantity of 7,7-bis(dimethylphenylphosphine)-*nido*-7-platinaundecaborane, $[(PhMe_2P)_2PtB_{10}H_{12}]$ (<1%, R_f 0.3) was isolated and subsequently identified by comparison of its n.m.r. parameters with those of authentic samples.[19–21]

(b) *With cis*-$[PtCl_2(PPh_3)_2]$. Following the procedure described in 1(a) above, using *cis*-$[PtCl_2(PPh_3)_2]$ (0.3 g, 0.38 mmol) instead of *cis*-$[PtCl_2(PMe_2Ph)_2]$ led to the isolation of $[Pt_2(\mu\text{-}\eta^3\text{-}B_6H_9)_2(PPh_3)_2]$ {23.5 mg, 22 μmol, 4.1%, R_f 0.88 [eluant light petroleum (b.p. 60—80 °C)—CH_2Cl_2 (40:60)], m.p. (decomp.) >200 °C}, $[(Ph_3P)_2PtB_8H_{12}]$ [54.3 mg, 66 μmol, 12.3%. R_f 0.75, m.p. (decomp.) 132—134 °C], $[(Ph_3P)_2PtB_{10}H_{12}]$ (9.1 mg, 11 μmol, 2.0%, R_f 0.75), and an unidentified platinaborane (<1%, R_f 0.87), possibly $[(Ph_3P)_2Pt_2B_8H_{14}]$ (see Results and Discussion, section 2).

(c) *With cis*-$[PtCl_2(PMe_2Ph)_2]$ *and tmnda ('proton sponge') in methanol in a* 1:1:2 *molar ratio.* 'Proton sponge' (0.16 g, 0.76 mmol) and *cis*-$[PtCl_2(PMe_2Ph)_2]$ (0.21 g, 0.38 mmol) were dissolved in MeOH (20 cm^3) and to this solution was added $6,6'$-$(B_{10}H_{13})_2O$ (0.1 g, 0.39 mmol) again dissolved in MeOH (30 cm^3). Instantly a vigorous reaction occurred with effervescence and an amber coloured solution resulted. The reaction subsided after *ca.* 5 min and an off-white precipitate was deposited over *ca.* 30 min. This material was collected by filtration, recrystallised from hot CH_2Cl_2–C_6H_{12} (20:80, *ca.* 30 cm^3) under N_2, and was identified[22] as $[(PhMe_2P)_2PtB_8H_{12}]$. The filtrate was reduced in volume under reduced pressure and $B(OMe)_3$ was identified in the volatile fraction. The reduced filtrates were separated by preparative scale t.l.c., light petroleum (b.p. 60—80 °C)—CH_2Cl_2 (1:1) as eluant, to yield small quantities of $[Pt_2(\mu\text{-}\eta^3\text{-}B_6H_9)_2(PMe_2Ph)_2]$ (3 mg, 3.7 μmol, *ca.* 1%) and a second crop of $[(PhMe_2P)_2PtB_8H_{12}]$ (0.17 g, 0.3 mmol, total yield 78%).

(d) *With cis*-$[NiCl_2(PMe_2Ph)_2]$. A repeat of the procedure described in 1(a) above using *cis*-$[NiCl_2(PMe_2Ph)_2]$ (0.16 g, 0.39 mmol) and using light petroleum (b.p. 60—80 °C)–CH_2Cl_2 (40:60) as eluant led to the isolation of $PhMe_2P{\cdot}BH_3$ (20 mg, 0.1 mmol, 34%, R_f 0.45), $PhMe_2P{\cdot}B_3H_7$ (61 mg, 0.33 mmol, 8.8%, R_f 0.80), and $PhMe_2P{\cdot}B_9H_{13}$ (27 mg, 0.1 mmol, 28.0%, R_f 0.75) which were identified by comparison of their n.m.r. parameters with published data.[53–55] Also a very small yield of a red crystalline nickelaborane, 2,4-dichloro-1,1-bis(dimethylphenylphosphine)-*closo*-1-nickeladecaborane (<1%, R_f 0.85) was isolated and recrystallised from CH_2Cl_2–Et_2O to yield red crystals, of which one was suitable for *X*-ray diffraction experiments.

(e) *With cis*-$[PdCl_2(PMe_2Ph)_2]$. A repeat of the procedure described in 1(a) above using *cis*-$[PdCl_2(PMe_2Ph)_2]$ (0.5 g, 1.1 mmol) and $6,6'$-$(B_{10}H_{13})_2O$ (0.28 g, 1.1 mmol), led to the isolation of $PhMe_2P{\cdot}BH_3$ (3 mg, 20 μmol, 2%), $PhMe_2P{\cdot}B_3H_7$ (3 mg, 17 μmol, 1.5%), and $PhMe_2P{\cdot}B_9H_{13}$ (9 mg, 36 μmol, 3.3%). Also isolated was $[(PhMe_2P)_2PdB_8H_{12}]$ {21 mg, 43 μmol, 4%, R_f 0.55 [eluant as in 1(d)]}. Finally, a small (<1%) amount of unstable red metallaborane was isolated but not identified (see Results and Discussion, section 4).

(f) *With cis*-$[PdCl_2(PPh_3)_2]$. A repeat of the procedure described in 1(a) using *cis*-$[PdCl_2(PPh_3)_2]$ (0.5 g, 0.7 mmol) and $6,6'$-$(B_{10}H_{13})_2O$ (0.19 g, 0.7 mmol), led to the isolation of $Ph_3P{\cdot}B_9H_{13}$ {9.5 mg, 25 μmol, 11%, R_f 0.7 [eluant as in 1(d)]}, $[(Ph_3P)_2PdB_8H_{12}]$ (26 mg, 36 μmol, 5.1%, R_f 0.8), $Ph_3P{\cdot}B_3H_7$ (trace), and a small quantity of unidentified red metallaborane analogous to that mentioned in 1(e) above.

2. *Reaction of* 6-$B_{10}H_{13}OH$ *with cis*-$[PtCl_2(PMe_2Ph)_2]$, *in a* 2:1 *molar ratio.* A mixture of *cis*-$[PtCl_2(PMe_2Ph)_2]$ (88 mg, 0.16 mmol) and 6-$B_{10}H_{13}OH$ (45 mg, 0.33 mmol) in CH_2Cl_2–Et_2O (1:1, *ca.* 10 cm^3) was stirred for *ca.* 72 h at room temperature. The resulting yellow solution was worked up and the products separated as described in 1(a) above. This led to the isolation of $[Pt_2(\mu\text{-}\eta^3\text{-}B_6H_9)_2(PMe_2Ph)_2]$ (5.3 mg, 6.5 μmol, 4.1%) and $[(PhMe_2P)_2PtB_8H_{12}]$ (16.5 mg, 29 μmol, 18%).

3. *Reactions of* $[NMe_4][B_9H_{14}]$ *with cis*-$[MCl_2L_2]$ (M = Pt, Pd, *or* Ni; L = PMe_2Ph, PPh_3, *or dppe*). (a) *cis*-$[PtCl_2(PPh_3)_2]$, *in a* 2:1 *molar ratio. cis*-$[PtCl_2(PPh_3)_2]$ (0.43 g, 0.55 mmol) was dissolved with $[NMe_4][B_9H_{14}]$ (0.2 g, 1.1 mmol) in CH_2Cl_2 (*ca.* 100 cm^3) and stirred for 16 h at room temperature. The volume was reduced to *ca.* 20 cm^3 under reduced pressure and filtered through silica gel [Kieselgel 60 (Merck); mesh 0.063—0.200 mm; *ca.* 5 g], at which point gas was evolved. The silica gel was washed with CH_2Cl_2 until the eluant was colourless, the combined eluants were reduced in volume, and separated by column chromatography, using CH_2Cl_2–C_6H_{12} (1:1, *ca.* 1 dm^3) as eluant. The minor product, $[Pt_2(\mu\text{-}\eta^3\text{-}B_6H_9)_2(PPh_3)_2]$ (23 mg, 22 μmol, 8%), was recrystallised from CH_2Cl_2–C_6H_{12} (1:4, *ca.* 10 cm^3) and the major product, $[(Ph_3P)_2PtB_8H_{12}]$ (0.29 g, 0.4 mmol, 65%), was recrystallised from hot CH_2Cl_2 (*ca.* 5 cm^3).

(b) *cis*-$[PtCl_2(PMe_2Ph)_2]$ *in methanol.* $[NMe_4][B_9H_{14}]$ (0.1 g, 0.54 mmol) and *cis*-$[PtCl_2(PMe_2Ph)_2]$ (0.29 g, 0.54 mmol) were dissolved separately in MeOH (20 cm^3 each) and on mixing a vigorous reaction occurred with effervescence. After 1 h a precipitated solid was filtered off and identified as $[(PhMe_2P)_2PtB_8H_{12}]$. The liquor was reduced in volume to *ca.* 10 cm^3 under reduced pressure, the volatile fraction containing $B(OMe)_3$. The remaining solution was separated by preparative scale t.l.c. using light petroleum (b.p. 60—80 °C)—CH_2Cl_2 (1:1) as eluant. The combined $[(PhMe_2P)_2PtB_8H_{12}]$ fractions (0.2 g, 0.4 mmol, 65%) were recrystallised from CH_2Cl_2–C_6H_{12} (1:4, *ca.* 10 cm^3) and a small quantity of $[Pt_2(\mu\text{-}\eta^3\text{-}B_6H_9)_2(PMe_2Ph)_2]$ (4.4 mg, 5.4 μmol, 1%) was also isolated.

(c) *cis*-$[NiCl_2(PMe_2Ph)_2]$, *in a* 2:1 *molar ratio.* The only isolable products from the reaction between *cis*-$[NiCl_2(PMe_2Ph)_2]$ and $[NMe_4][B_9H_{14}]$ were phosphinoboranes and no further work was carried out on this reaction.

(d) $[NiCl_2(dppe)]$, *in a* 2:1 *molar ratio.* $[NiCl_2(dppe)]$ (0.05 g,

0.1 mmol) and $[NMe_4][B_9H_{14}]$ (0.037 g, 0.2 mmol) in CH_2Cl_2 (*ca.* 100 cm^3) were heated under reflux for *ca.* 24 h. After this time the reaction mixture was filtered and reduced in volume. Preparative scale t.l.c. using CH_3CN–C_6H_{14}–CH_2Cl_2 (1:6:3) *as eluant led* to the isolation of one component tentatively identified (Table 10) as $[(dppe)NiB_8H_{12}]$ (*ca.* 5%, R_f 0.4).

(e) *cis*-$[PdCl_2(PMe_2Ph)_2]$, *in a* 2:1 *molar ratio.* Following the procedure described in 3(a) above using $[NMe_4][B_9H_{14}]$ (0.1 g, 0.54 mmol) and *cis*-$[PdCl_2(PMe_2Ph)_2]$ (0.12 g, 0.27 mmol) led to the isolation of four components: $PhMe_2P{\cdot}BH_3$ (5.4 mg, 35 μmol, 6.6%), $PhMe_2P{\cdot}B_3H_7$ (6.2 mg, 35 μmol, 6.6%), $PhMe_2P{\cdot}B_9H_{13}$ (11.6 mg, 47 μmol, 8.6%), and $[(PhMe_2P)_2PdB_8H_{12}]$ (39 mg, 81 μmol, 32%).

Reactions of $[(PhMe_2P)_2PtB_8H_{12}]$.—(a) With KH *and cis*-$[PdCl_2(PMe_2Ph)_2]$, *in a* 1:2:1 *molar ratio.* CH_2Cl_2–thf (1:1, *ca.* 20 cm^3) was distilled into a flask containing $[(PhMe_2P)_2PtB_8H_{12}]$ (0.1 g, 0.18 mmol) at −198 °C. To this was added KH (70% active, 0.024 g, corresponding to 0.36 mmol KH) *via* a side-arm tube and the flask was allowed to warm to room temperature, upon which effervescence occurred and the solution gradually turned yellow. After *ca.* 15 min *cis*-$[PdCl_2(PMe_2Ph)_2]$ (0.08 g, 0.18 mmol) was added and the mixture stirred for *ca.* 1 h. The solvent was removed under reduced pressure and the residual solid was separated into three components using preparative scale t.l.c. with CH_2Cl_2 as eluant. The components were $[(PhMe_2P)_2PtB_8H_{12}]$ (9.6 mg, 17 μmol, 12%, R_f 0.85), $[(PhMe_2P)_4Pt_2B_8H_{10}]$ (5.6 mg, 5.4 μmol, 3%, R_f 0.35), and $[(PhMe_2P)_4PdPtB_8H_{10}]$ (34 mg, 36 μmol, 20%, R_f 0.50). $[(PhMe_2P)_4PdPtB_8H_{10}]$ yielded orange crystals after recrystallisation from C_6H_{12}–CH_2Cl_2 (4:1; *ca.* 20 cm^3).

(b) *With* KH *and other transition metal complexes, in a* 1:2:1 *molar ratio.* The procedure described in (a) above was essentially repeated using the following complexes (0.18 mmol): $[CuCl(PPh_3)_3]$*, $[CuCl(PMe_2Ph)_3]$, $[FeBr_2(CO)_4]$, $[IrCl(CO)(PPh_3)_2]$*, $[RhCl(CO)(PPh_3)_2]$*, $[Fe(C_5H_5)(CO)_2I]$, and *cis*-$[NiCl_2(PMe_2Ph)_2]$. These reactions produced no significant yields of any new dimetallaboranes. However, one new species was generated in some of these reactions (with the complexes marked *) as a result of ligand exchange. This was $[(PhMe_2P)(Ph_3P)PtB_8H_{12}]$ (< 2 mg, *ca.* R_f 0.88). Other typical yields were: $[(PhMe_2P)_2PtB_8H_{12}]$ (6.2—9.2 mg, 6—9% recovery), $[(PhMe_2P)_4Pt_2B_8H_{10}]$ (< 4 mg, 1—4%), and $[(Ph_3P)_2PtB_8H_{12}]$ (6—7 mg, 4—5%) (a known compound; also from ligand exchange).

Reaction of $[Pt_2(\mu\text{-}\eta^3\text{-}B_6H_9)_2(PMe_2Ph)_2]$.—(a) *With* KH *and cis*-$[PtCl_2(PMe_2Ph)_2]$, *in a* 1:1:1 *molar ratio.* CH_2Cl_2–thf (1:1, 30 cm^3) was distilled into a flask containing $[Pt_2(\mu\text{-}\eta^3\text{-}B_6H_9)_2(PMe_2Ph)_2]$ (0.05 g, 60 μmol) at −196 °C. To this was added KH (70% active, 3.5 mg; corresponding to 60 μmol KH) *via* a side-arm tube. The flask was allowed to warm to room temperature, upon which effervescence occurred and the solution gradually turned orange. After *ca.* 15 min *cis*-$[PtCl_2(PMe_2Ph)_2]$ (0.033 g, 60 μmol) was added and the mixture left to stir at room temperature for *ca.* 1 h. The solvent was then removed under reduced pressure and the residue was extracted with CH_2Cl_2 (20 cm^3). This solution was then separated by preparative scale t.l.c. using light petroleum (b.p. 60—80 °C)—CH_2Cl_2 (1:1) as eluant. Two mobile components were isolated $[Pt_2(\mu\text{-}\eta^3\text{-}B_6H_9)_2(PMe_2Ph)_2]$ (30 mg, 37 μmol, 60% recovery, R_f 0.42) and $[Pt_2(\mu\text{-}\eta^3\text{-}B_6H_9)(\mu\text{-}\{\eta^3\text{-}B_6H_8\text{-}\eta^2\text{-}[PtH(PMe_2Ph)_2]\})(PMe_2Ph)_2]$ (7.7 mg, 6 μmol, 10%, R_f 0.2), identified as described in the Results and Discussion, section 6.

(b) *With tmnda ('proton sponge') and cis*-$[PtCl_2(PMe_2Ph)_2]$, *in a* 1:1:1 *molar ratio.* A similar procedure to that described in (a) above was followed using 'proton sponge' (12.8 mg, 0.06 mmol) in place of the KH, with subsequent heating of the solution under reflux for 1 h. Work-up of the resulting solution, as described in (a), yielded $[Pt_2(\mu\text{-}\eta^3\text{-}B_6H_9)_2(PMe_2Ph)_2]$ (6 mg, 7.4 μmol, 12% recovery) and $[Pt_2(\mu\text{-}\eta^3\text{-}B_6H_9)(\mu\text{-}\{\eta^3\text{-}B_6H_8\text{-}\eta^2\text{-}[PtH(PMe_2Ph)_2]\})(PMe_2Ph)_2]$ (3.9 mg, 3 μmol, 5%).

(c) *With* KH *and other transition metal complexes.* The basic procedure described in (a) above was followed replacing the *cis*-$[PtCl_2(PMe_2Ph)_2]$ with 60 μmol of the following complexes: $[CuCl(PMe_2Ph)_3]$, $[CuCl(PPh_3)_3]$*, $[IrCl(CO)(PPh_3)_2]$*, and $[Fe(C_5H_5)(CO)_2I]$. No new trimetallaboranes were produced in these reactions, but one new species was generated in some of these reactions (with the complexes marked *) as a result of ligand exchange. This was $[Pt_2(\mu\text{-}\eta^3\text{-}B_6H_9)_2(PMe_2Ph)(PPh_3)]$ (1.1 mg, 1.2 μmol, 2%, R_f 0.44). Other typical yields were: $[Pt_2(\mu\text{-}\eta^3\text{-}B_6H_9)_2(PMe_2Ph)_2]$ (2.5—4 mg, 3—5 μmol, 5—8% recovery), and $[Pt_2(\mu\text{-}\eta^3\text{-}B_6H_9)_2(PPh_3)_2]$ (3—4 mg, 3—4 μmol, 5—6%) (a known compound; also due to ligand exchange).

X-*Ray Analysis of* $[Pt_2(\mu\text{-}\eta^3\text{-}B_6H_9)_2(PMe_2Ph)_2]$.— *Crystal data.* $C_{16}H_{40}B_{12}P_2Pt_2$, M = 814.34, monoclinic, a = 1 014.0(2), b = 586.8(2), c = 2 316.9(6) pm, β = 91.66(2)°, U = 1.378(1) nm^3, Z = 2, D_c = 1.962 g cm^{-3}, $F(000)$ = 764, space group $P2_1/c$, Mo-K_α radiation, graphite monochromatised, λ = 71.069 pm, μ(Mo-K_α) = 103.7 cm^{-1}.

Structure determination. Cell dimensions were determined by least-squares treatment of the setting angles of 15 reflections with $35 < 2\theta < 40°$. Intensities of the 2 426 independent reflections having $2\theta < 50°$ were measured in the θ—2θ scan mode, and after correction for Lorentz, polarisation, and absorption factors the 2 234 reflections with $I > 3\sigma(I)$ were retained for the structure analysis. Absorption effects were severe, the crystal being a thin plate of dimensions 0.56 × 0.29 × 0.05 mm, and the resulting transmission factors range from 0.069 to 0.585. Solution from Patterson and difference syntheses was followed by full-matrix least-squares refinement. An initial refinement with isotropic thermal parameters for all the non-hydrogen atoms converged to an R of 0.171 without absorption corrections, reducing to R = 0.046 when absorption corrections were included. With anisotropic thermal parameters for all the non-hydrogen atoms and with a weighting scheme derived from $\sigma^2(I) = \sigma_c^2(I) + (0.02I)^2$, where σ_c^2 is the variance from counting statistics, convergence occurred at R = 0.037, R' = 0.050. In a final-difference map many of the hydrogen atoms appeared, but some of the borane hydrogen atoms were not well defined, and so none of the hydrogen atoms was included. The final atomic co-ordinates and their standard deviations are given in Table 22. For deposited supplementary data see ref. 7.

X-*Ray Analysis of* $[(PhMe_2P)_2NiB_9H_7Cl_2]$.—*Crystal data.* $C_{16}H_{29}B_9Cl_2NiP_2$, M = 510.26, monoclinic, a = 1 341.2(2), b = 1 321.5(2), c = 1 476.3(2) pm, β = 109.50(1)°, U = 2.466 6(7) nm^3, Z = 4, D_c = 1.374 g cm^{-3}, $F(000)$ = 1 048, space group $C2/c$, Mo-K_α radiation, λ = 71.069 pm, μ(Mo-K_α) = 11.40 cm^{-1}.

Structure determination. Cell dimensions were obtained as for the previous compound. Intensities of the 1 623 independent reflections to 2θ = 45° were measured in the θ—2θ scan mode and after correction for Lorentz, polarisation, and transmission factors the 1 530 reflections having $I > 2\sigma(I)$ were retained for the structure analysis. Solution from Patterson and difference syntheses, followed by anisotropic refinement of all the non-hydrogen atoms converged at R = 0.05. Calculations used the SHELX programs,[68] and the phenyl rings were constrained as regular hexagons with C–C = 139.5 pm. Inclusion of the phenyl and methyl hydrogens in idealised positions with C–H = 108 pm reduced R to 0.0395. A difference map now revealed the four independent borane hydrogens as the largest peaks, with

Table 22. Atomic co-ordinates for $[Pt_2(\mu\text{-}\eta^3\text{-}B_6H_9)_2(PMe_2Ph)_2]$ with estimated standard deviations in parentheses

Atom	*x*	*y*	*z*
Pt(1)	0.081 56(2)	0.098 75(5)	0.037 87(1)
P(1)	0.217 00(16)	0.297 92(36)	0.101 36(8)
C(1)	0.270 9(8)	0.127 5(13)	0.163 3(4)
C(2)	0.391 1(7)	0.013 0(15)	0.163 3(4)
C(3)	0.430 2(10)	−0.131 4(17)	0.208 3(5)
C(4)	0.348 8(11)	−0.149 5(17)	0.255 0(5)
C(5)	0.230 9(11)	−0.039 3(18)	0.256 1(4)
C(6)	0.192 2(10)	0.099 9(15)	0.210 7(4)
C(7)	0.370 7(8)	0.422 0(14)	0.076 0(4)
C(8)	0.147 3(9)	0.553 3(13)	0.133 0(4)
B(1)	−0.249 6(9)	0.117 3(16)	0.080 2(4)
B(2)	−0.261 2(9)	−0.025 7(17)	0.011 6(5)
B(3)	−0.127 9(7)	0.172 1(15)	0.025 5(4)
B(4)	−0.078 0(9)	0.137 3(18)	0.101 3(5)
B(5)	−0.180 3(11)	−0.077 6(18)	0.130 6(5)
B(6)	−0.295 4(10)	−0.171 4(20)	0.078 3(5)

Table 23. Atomic co-ordinates for $[1,1\text{-}(PhMe_2P)_2\text{-}2,4\text{-}Cl_2\text{-}closo\text{-}1\text{-}NiB_9H_7]$ with estimated standard deviations in parentheses

Atom	*x*	*y*	*z*
Ni(1)	0	0.143 32(3)	$\frac{1}{4}$
P	−0.003 05(6)	0.248 86(5)	0.369 37(5)
Cl	0.220 48(6)	0.085 63(6)	0.347 95(6)
B(2)	0.095 5(3)	0.022 9(2)	0.294 6(2)
B(3)	0.018 8(3)	0.021 1(2)	0.166 9(2)
H(3)	0.038 4(25)	0.038 8(25)	0.103 7(25)
B(6)	0.085 0(3)	−0.089 7(3)	0.225 5(3)
H(6)	0.158 6(26)	−0.112 6(27)	0.211 3(24)
B(9)	0.057 3(3)	−0.090 2(3)	0.341 8(3)
H(9)	0.104 7(28)	−0.118 1(26)	0.409 9(26)
B(10)	0	−0.172 9(4)	$\frac{1}{4}$
H(10)	0	−0.254 8(39)	$\frac{1}{4}$
C(1)	0.043 6(1)	0.377 5(1)	0.369 0(1)
C(2)	−0.0193	0.4615	0.3693
C(3)	0.0230	0.5588	0.3753
C(4)	0.1281	0.5720	0.3810
C(5)	0.1909	0.4880	0.3806
C(6)	0.1487	0.3908	0.3746
C(7)	−0.135 8(2)	0.259 3(2)	0.375 7(3)
C(8)	0.078 1(2)	0.209 0(2)	0.489 2(2)

The phenyl group (with hydrogens) was refined as a rigid group. C(2)—C(6) and the attached hydrogens have the same e.s.d.s as C(1).

heights of 0.60—0.74 e Å^{-3}. After inclusion and refinement of these hydrogen atoms (with fixed U_{iso} of 700 pm^2) convergence was reached at $R = 0.0295$, $R' = 0.0404$. The final atomic co-ordinates and estimated standard deviations are in Table 23.

Acknowledgements

We thank Dr. P. Gans for obtaining the Raman spectrum of $[Pt_2(\mu\text{-}\eta^3\text{-}B_6H_9)_2(PMe_2Ph)_2]$, Mr. A. Hedley for microanalyses, Mr. D. Singh for mass spectrometry, and the S.E.R.C. for financial support, including a maintenance grant (to M. J. H.).

References

1 Gmelin Handbuch der Anorganischen Chemie Erganzungswerk zur 8 Auflage Band 54, Borverbindungen Teil 20, Springer-Verlag, Berlin, 1979.
2 S. G. Shore, in 'Boron Hydride Chemistry,' ed. E. L. Muetterties, Academic Press, New York, 1975, ch. 3, p. 79.
3 S. Heřmánek, J. Plešek, and B. Štíbr, *Collect. Czech. Chem. Commun.*, 1968, **33**, 691.
4 J. D. Kennedy and N. N. Greenwood, *Inorg. Chim. Acta*, 1980, **38**, 93.
5 N. N. Greenwood, W. S. McDonald, and T. R. Spalding, *J. Chem. Soc., Dalton Trans.*, 1980, 1251; E. L. Muetterties, J. H. Balthis, Y. T. Chia, W. H. Knoth, and H. C. Miller, *Inorg. Chem.*, 1964, **3**, 444.
6 N. N. Greenwood, J. D. Kennedy, and D. Taylorson, *J. Phys. Chem.*, 1978, **82**, 623.
7 N. N. Greenwood, M. J. Hails, J. D. Kennedy, and W. S. McDonald, *J. Chem. Soc., Chem. Commun.*, 1980, 37.
8 R. M. Adams, *Pure Appl. Chem.*, 1972, **30**, 683.
9 F. Hanousek, Z. Samek, and P. Sedmera, *Collect. Czech. Chem. Commun.*, 1968, **33**, 2169.
10 R. F. Sprecher, B. E. Aufderheide, G. W. Luther, and J. C. Carter, *J. Am. Chem. Soc.*, 1974, **96**, 4404.
11 R. F. Sprecher and J. C. Carter, *J. Am. Chem. Soc.*, 1973, **95**, 2369.
12 A. R. Siedle, D. McDowell, and L. J. Todd, *Inorg. Chem.*, 1974, **13**, 2735.
13 J. D. Kennedy, in 'NMR in Inorganic and Organometallic Chemistry,' ed. J. Mason, Plenum Press, 1985, ch. 8 and refs. therein.
14 S. Heřmánek, J. Plešek, and B. Štíbr, *Collect. Czech. Chem. Commun.*, 1966, **31**, 4744; 1969, **34**, 194.
15 F. Klanberg, E. L. Muetterties, G. W. Parshall, and P. A. Wegner, *Inorg. Chem.*, 1968, **7**, 2072.
16 N. N. Greenwood and J. D. Kennedy, in 'Metal Interactions with Boron Clusters,' ed. R. N. Grimes, Plenum Press, New York, 1982, ch. 2, pp. 43—118.
17 N. N. Greenwood, J. D. Kennedy, and J. Staves, *J. Chem. Soc., Dalton Trans.*, 1978, 1146.
18 J. D. Kennedy and J. Staves, *Z. Naturforsch., Teil B.*, 1979, **34**, 808.
19 J. D. Kennedy and B. Wrackmeyer, *J. Magn. Reson.*, 1980, **38**, 529.
20 S. K. Boocock, N. N. Greenwood, and J. D. Kennedy, *J. Chem. Soc., Chem. Commun.*, 1980, 305.
21 S. K. Boocock, N. N. Greenwood, J. D. Kennedy, W. S. McDonald, and J. Staves, *J. Chem. Soc., Dalton Trans.*, 1981, 2573.
22 S. K. Boocock, N. N. Greenwood, M. J. Hails, J. D. Kennedy, and W. S. McDonald, *J. Chem. Soc., Dalton Trans.*, 1981, 1415.
23 Y. M. Cheek, N. N. Greenwood, J. D. Kennedy, and W. S. McDonald, *J. Chem. Soc., Chem. Commun.*, 1982, 80.
24 (*a*) M. A. Beckett, J. E. Crook, N. N. Greenwood, J. D. Kennedy, and W. S. McDonald, *J. Chem. Soc., Chem. Commun.*, 1982, 552; (*b*) M. A. Beckett, J. E. Crook, N. N. Greenwood, and J. D. Kennedy, *ibid.*, 1983, 1228.
25 R. Ahmad, J. E. Crook, N. N. Greenwood, J. D. Kennedy, and W. S. McDonald, *J. Chem. Soc., Chem. Commun.*, 1982, 1019.
26 J. E. Crook, N. N. Greenwood, J. D. Kennedy, and W. S. McDonald, *J. Chem. Soc., Dalton Trans.*, 1984, 2487.
27 N. N. Greenwood, J. D. Kennedy, W. S. McDonald, and D. Reed, *J. Chem. Soc., Dalton Trans.*, 1979, 117.
28 N. N. Greenwood, J. D. Kennedy, and D. Reed, *J. Chem. Soc., Dalton Trans.*, 1980, 196.
29 S. K. Boocock, J. Bould, N. N. Greenwood, J. D. Kennedy, and W. S. McDonald, *J. Chem. Soc., Dalton Trans.*, 1982, 713.
30 J. E. Crook, N. N. Greenwood, J. D. Kennedy, and W. S. McDonald, *J. Chem. Soc., Chem. Commun.*, 1981, 933.
31 J. Bould, N. N. Greenwood, and J. D. Kennedy, *J. Chem. Soc., Dalton Trans.*, 1982, 481.
32 J. Bould, J. E. Crook, N. N. Greenwood, J. D. Kennedy, and W. S. McDonald, *J. Chem. Soc., Chem. Commun.*, 1982, 346.
33 J. E. Crook, N. N. Greenwood, J. D. Kennedy, and W. S. McDonald, *J. Chem. Soc., Chem. Commun.*, 1982, 383.
34 J. Bould, N. N. Greenwood, J. D. Kennedy, and W. S. McDonald, *J. Chem. Soc., Chem. Commun.*, 1982, 465.
35 J. E. Crook, N. N. Greenwood, J. D. Kennedy, and W. S. McDonald, *J. Chem. Soc., Chem. Commun.*, 1983, 83.
36 (*a*) J. Bould, J. E. Crook, N. N. Greenwood, and J. D. Kennedy, *J. Chem. Soc., Dalton Trans.*, 1984, 1903; (*b*) J. Bould, N. N. Greenwood, and J. D. Kennedy, *ibid.*, p. 2477.
37 (*a*) J. Bould, N. N. Greenwood, and J. D. Kennedy, *J. Organomet. Chem.*, 1983, **249**, 11; (*b*) J. E. Crook, M. Elrington, N. N. Greenwood, J. D. Kennedy, M. Thornton-Pett, and J. D. Woollins, *J. Chem. Soc., Dalton Trans.*, submitted for publication.
38 (*a*) R. Ahmad, M. A. Beckett, J. Bould, Y. M. Cheek, J. E. Crook, N. N. Greenwood, and J. D. Kennedy, unpublished work; (*b*) M. A. Beckett, J. E. Crook, N. N. Greenwood, and J. D. Kennedy, *J. Chem. Soc., Dalton Trans.*, 1984, 1427; (*c*) M. A. Beckett, N. N. Greenwood, J. D. Kennedy, and M. Thornton-Pett, *ibid.*, in the press.

39 J. P. Brennan, A. Davison, R. Schaeffer, and S. S. Wreford, *J. Chem. Soc., Chem. Commun.*, 1973, 354.
40 A. Davison, D. D. Traficante, and S. S. Wreford, *J. Am. Chem. Soc.*, 1974, **96**, 2802.
41 S. G. Shore, Proc. 19th Int. Conf. Coord. Chem., Prague, September, 1978, vol. 1, pp. 86—88.
42 N. M. Boag, J. Browning, C. Crocker, P. L. Goggin, R. J. Goodfellow, M. Murray, and J. L. Spencer, *J. Chem. Res.*, 1978, (*S*) 228.
43 A. Kühn and H. Werner, *Angew. Chem.*, 1977, **89**, 427.
44 D. J. Brauer, A. Kühn, C. Krüger, J. C. Sekutowski, Y. H. Tsay, D. J. Tune, and H. Werner, *Chem. Ber.* 1977, **110**, 1763.
45 J. C. Huffman, D. C. Moody, and R. Schaeffer, *Inorg. Chem.*, 1981, **20**, 741.
46 R. E. Enrione, F. P. Boer, and W. N. Lipscomb, *J. Am. Chem. Soc.*, 1964, **84**, 1451; *Inorg. Chem.*, 1964, **3**, 1659.
47 G. S. Pawley, *Acta Crystallogr.*, 1966, **20**, 631.
48 A. J. Stone and M. J. Alderton, *Inorg. Chem.*, 1981, 2297 and refs. therein.
49 D. A. Dixon, D. A. Kleier, T. A. Halgren, and W. N. Lipscomb, *J. Am. Chem. Soc.*, 1976, **98**, 2086.
50 J. C. Huffman, D. C. Moody, and R. Schaeffer, *J. Am. Chem. Soc.*, 1975, **97**, 1621.
51 J. D. Kennedy, I. J. Colquhoun, W. McFarlane, and R. J. Puddephatt, *J. Organomet. Chem.*, 1979, **172**, 479.
52 I. J. Colquhoun, J. D. Kennedy, and W. McFarlane, unpublished work.
53 A. H. Cowley and M. C. Damasco, *J. Am. Chem. Soc.*, 1971, **93**, 6815.
54 B. M. Graybill and J. K. Ruff, *J. Am. Chem. Soc.*, 1962, **84**, 1062.
55 G. M. Bodner, F. R. Scholer, L. J. Todd, L. E. Senor, and J. C. Carter, *Inorg. Chem.*, 1971, **10**, 942.
56 E. Walter and R. Schaeffer, *Inorg. Chem.*, 1973, **12**, 2209.
57 A. Bonny, J. R. Bowser, R. N. Grimes, and J. R. Pipal, *J. Am. Chem. Soc.*, 1979, **101**, 6229.
58 M. F. Hawthorne and R. N. Leyden, *J. Chem. Soc., Chem. Commun.*, 1975, 310.
59 R. D. Dobrott and W. N. Lipscomb, *J. Chem. Phys.*, 1962, **37**, 1779.
60 A. J. Welch, *J. Chem. Soc., Dalton Trans.*, 1976, 225.
61 M. Green, J. L. Spencer, and F. G. A. Stone, *J. Chem. Soc., Dalton Trans.*, 1979, 1679.
62 J. D. Kennedy, *Proc. 19th Int. Conf. Coord. Chem.*, Prague, September, 1978, **1**, 79.
63 J. D. Kennedy, *Prog. Inorg. Chem.*, 1984, **32**, 519.
64 G. R. Eaton and W. N. Lipscomb, 'NMR Studies of Boron Hydrides and Related Compounds,' W. A. Benjamin, New York and Amsterdam, 1969.
65 See, for example. G. W. Parshall, *Inorg. Synth.*, 1970, **12**, 26 and following papers.
66 N. N. Greenwood, J. D. Kennedy, T. R. Spalding, and D. Taylorson, *J. Chem. Soc., Dalton Trans.*, 1979, 840.
67 T. C. Gibb and J. D. Kennedy, *J. Chem. Soc., Faraday Trans. 2*, 1982, 525.
68 G. M. Sheldrick, SHELX system of programs, University of Cambridge, 1976.

Received 12*th June* 1984; *Paper* 4/988